5-2017

Hydrocarbon and CO_2 Emissions from Oil and Gas Production Well Pad Soils Comparative to Background Soil Emissions in Eastern Utah

Cody S. Watkins
Utah State University

HYDROCARBON AND CO_2 EMISSIONS FROM OIL AND GAS PRODUCTION WELL PAD SOILS COMPARATIVE TO BACKGROUND SOIL EMISSIONS IN EASTERN UTAH

by

Cody S. Watkins

A thesis submitted in partial fulfillment
of the requirements for the degree

of

MASTER OF SCIENCE

in

Geology

Approved:

_____	_____
Benjamin Burger, Ph.D. Major Professor	Seth Lyman, Ph.D. Committee Member
_____	_____
Dennis Newell, Ph.D. Committee Member	Mark McLellan, Ph.D. Vice President for Research and Dean of the School of Graduate Studies

UTAH STATE UNIVERSITY
Logan, Utah

2017

ABSTRACT

Hydrocarbon and CO_2 Emissions from Oil and Gas Production Well Pad Soils

Comparative to Background Soil Emissions in Eastern Utah

by

Cody Watkins, Master of Science

Utah State University, 2017

Major Professor: Dr. Benjamin Burger
Department: Geology

Emissions of methane, non-methane hydrocarbons (NMHC), and carbon dioxide (CO_2) at 27 natural gas well pads, 11 non-well locations in oil and gas fields, and 7 hydrocarbon-bearing outcrops in eastern Utah between 2013 and 2016 were measured using a dynamic flux chamber (DFC) in effort to answer the following questions: What effect does the development of oil and gas have on the observed air quality (increased ozone, CO_2, volatile organic compounds (VOCs), and/or methane emissions) in northeastern Utah? What percentage of these gases is due to natural background emissions, and what percentage is due to oil and gas development in the region? Methane emissions were the focus of this study, but emissions of other compounds were also measured to better understand the sources and characteristics of emissions. Background methane fluxes were all <1 milligram (mg) meter $(m)^{-2}$ hour $(h)^{-1}$. Methane emissions from well pad soils were commonly higher closer to the wellhead, though exceptions existed. Methane fluxes from well pad soils ranged from -5.6 to 70,000 mg m^{-2} h^{-1}. Based on analysis of NMHC emissions data, emissions from 68% of the sampled well pad soils

were due to leaks of raw natural gas, whereas the remaining emissions were likely from a combination of raw gas leaks, liquid hydrocarbon spills, and/or methanogenic processes. CO_2 emissions were higher than methane emissions 92% of the time at well sites, possibly due to CO_2 in natural gas, and/or CO_2 emitted from bacterial decomposition of soil organic matter and/or fossil hydrocarbons. Total combustible soil gas concentrations were measured at 21 wells. In summer 2015, soil properties were also analyzed to better understand well leakage. Wells categorized as shut-in had the highest average methane fluxes. Measured methane soil emissions were scaled-up for the entire Uinta Basin to estimate the overall emission from well pad soils, and to compare soil emissions with other natural gas-related sources. Producing and shut-in gas wells were estimated to emit 16.1 ± 4.3 and 8.6 ± 3.2 (90% confidence interval) t y^{-1} (tonne/year) of methane in the Uinta Basin, respectively, which is <0.1% of total methane emissions from all natural gas sources.

(75 pages)

PUBLIC ABSTRACT

Hydrocarbon and CO_2 Emissions near the Wellhead of Oil and Gas Production Sites Comparative to Background Emissions in Eastern Utah

Cody Watkins

What effect does the development of oil and gas have on the observed air quality (i.e., increased ozone, carbon dioxide (CO_2), volatile organic compounds (VOCs), and/or methane emissions) in northeastern Utah? What percentage of these gases is natural background emissions, and what percentage is due to the recent oil and gas development in the region? Emissions in this text refer to gases released from the earth's surface to the atmosphere. Methane is the primary compound in natural gas. Natural gas is a naturally occurring hydrocarbon gas mixture. Emissions of methane, non-methane hydrocarbons (NMHC), and CO_2 at 27 natural gas well pads, 11 non-well locations in oil and gas fields, and seven hydrocarbon-bearing outcrops in eastern Utah between 2013 and 2016 were measured. Emission measurements were collected using a dynamic flux chamber (DFC). Methane emissions were the focus of this study, but emissions of other compounds were also measured to better understand the sources and characteristics of methane emissions. Background methane fluxes were all <1 milligram (mg) meter (m)$^{-2}$ hour (h)$^{-1}$. Methane emissions from well pad soils were commonly higher closer to the wellhead, though exceptions existed. Methane flux from well pad soils ranged from -5.6 to 70,000 mg m^{-2} h^{-1}, though 81% of sampled well pad soils had fluxes <10 mg m^{-2} h^{-1}. Based on analysis of non-methane hydrocarbons (NMHC) emission data, emissions from 68% of the

sampled well pad soils were due to leaks of raw natural gas. The sources of emissions from the remaining well pad soils were likely a combination of raw gas leaks, liquid hydrocarbon spills, and/or methanogenic processes. CO_2 emissions were higher than methane emissions 92% of the time at well sites. CO_2 emissions could have originated from leaking CO_2 in natural gas, or CO_2 emitted from bacterial decomposition of organic matter in the soil. Total combustible soil gas is the amount of hydrocarbon gases that are present in the interstitial space of soil. Total combustible soil gas concentrations were measured at 21 wells. Combustible soil gas concentrations and methane emissions were poorly correlated. Soil gas and emissions measurement locations were nearby but not identical, and the poor correlations could be due to non-uniform distributions of measured gases in the soil. In summer 2015, soil properties were also analyzed to understand emissions better. At well sites, low soil pH and high total organic carbon content were associated with increased methane emissions. Wells categorized as shut-in had the highest average methane flux. Measured methane soil emissions were scaled-up for the entire Uinta Basin to estimate the overall emission from well pad soils, and to compare soil emissions with other natural gas-related sources. Methane emissions from natural gas facilities have been previously quantified. Emission measurements from this study were compared against other emission sources at natural gas facilities to estimate the significance leaking wells have on air quality. The status of the well can change throughout the lifetime of a well. Producing and shut-in gas wells were estimated to emit 16.1 ± 4.3 and 8.6 ± 3.2 (90% confidence interval) t y^{-1} (tonne/year) of methane in the Uinta Basin, respectively, which is <0.1% of total methane emissions from all natural gas sources.

ACKNOWLEDGMENTS

Many people have encouraged me throughout this project that I would like to thank. I would first like to thank Seth Lyman for continual guidance, suggestions, and expertise in this field of study. He spent many hours to help with my plan of research, instrumentation use, and regular meetings to direct me in this project. I would like to thank Benjamin Burger, my advisor, who has been encouraging, supportive and has led me to meet academic requirements. I appreciate Dennis Newell and his encouragement, ideas, and his initial support in directing my research as an undergraduate student. I thank the U.S. Geological Survey for installing soil gas probes. I am grateful for the oil and gas companies that have allowed us to sample on their well pads. The Department of Geology at Utah State University has been a great support throughout my education. Much appreciation goes to the USU Bingham Research Center Team that has supported me in the field, laboratory, meetings, and conferences. I would especially like to thank my wife Chelsey for her strong encouragement and support throughout this project and for taking care of our two children, Ross and Ella, while I was pursuing my education. I give special thanks to my parents for supporting me throughout my education. This project has made me a better person and scientist.

Funding, project scope, and federal well locations for this project were provided by the Bureau of Land Management (Cooperative Agreement No. L13AC00292). Additional funding was provided by the Research of Secure Energy for America and Department of Energy (Contract No. 12122-15).

Cody S. Watkins

CONTENTS

Page

LIST OF TABLES

LIST OF FIGURES

CHAPTER 1

INTRODUCTION

1.1 Overview

Growing concern over an increase in atmospheric methane and carbon dioxide (CO_2) and their role in climate change has led to a number of studies to determine the rates of emissions of these compounds from oil and gas exploration and production (e.g., Howarth, 2011). Furthermore, methane and non-methane hydrocarbons (NMHC), including alkanes, alkenes, and aromatics, can react with other atmospheric pollutants to create ozone (Edwards, 2013). Ozone is harmful to humans and a major contributor to poor air quality (Chen, 2007; Conley 2016).

In this study, methane, NMHC, and CO_2 emissions were measured using a dynamic flux chamber (DFC) at 27 oil and gas well sites in eastern Utah, including wells in Paradox Basin, Uinta Basin, and Clay Basin. Emissions from non-well soil surfaces within oil and gas fields and hydrocarbon-bearing outcrops were also measured. The non-well sites were used to help establish background flux values to compare against emission from well sites. Concentrations of total combustible gas in soil, chemical and physical properties of soil, meteorological conditions, well properties (geology and well construction/status), and the sample location distance from the wellhead, were analyzed in relation to emissions fluxes to help determine the transport mechanisms and source(s) of measured emissions.

1.2 Objective

The objective of this study was to quantify CO_2, methane, and NMHC emissions from soils at natural gas production sites and hydrocarbon-bearing outcrops. At natural

gas production sites, sources of methane and NMHC emissions may be due to 1) poor design or construction of a gas well, which could allow hydrocarbon migration to the surface, 2) emissions from liquid hydrocarbon spills, or 3) bacterial methane production. At non-well sites, emissions may be due to 1) surface geologic features that directly emit CO_2 and hydrocarbons (Kirchgessner, 2000); 2) migration pathways, such as geologic faults, that allow these gases to reach the surface from subsurface reservoirs (Selley, 1997); or 3) bacterial methane production (Leson and Winer, 1991). Correlations of fluxes with total combustible soil gas, well properties, meteorology, and soil properties were examined to help determine the transport mechanisms and source(s) of emissions.

1.3 Significance

Characterization of emissions at oil and gas production sites is needed to understand the potential impact oil and gas wells may have on climate change and air quality (Kang, 2014; Allen, 2013). When methane escapes into the atmosphere, the short-term contribution to the greenhouse effect and global warming is 34 times more powerful than CO_2 (Brownstein, 2013; Davies, 2014). Brandt (2014) suggested that natural gas and oil operations are significant contributors to increased methane concentrations in the atmosphere. Energy companies are making improvements in drilling and infrastructure to decrease the amount of methane emissions that originate from natural gas wells, both voluntarily and due to increased regulatory requirements (EPA, 2016). Identification of leaks and/or spills at production sites allows operators to make changes that will increase production and reduce emissions. Well site soil emissions above background levels were categorized as raw natural gas leaks or re-emissions from liquid hydrocarbon spills.

The Uinta Basin in eastern Utah experiences strong inversions during winter months. The inversions trap hydrocarbons and other compounds that react to produce ozone. NMHC and nitrogen oxide (NO_x) react in the presence of sunlight to form ozone (Edwards, 2013). Ozone is an air pollutant that impacts lung health, especially for those with asthma or other lung conditions (Chen, 2007; Conley 2016). In October 2015, the Environmental Protection Agency (EPA) lowered the ground-level ozone limit from 75 to 70 ppbv (parts per billion by volume) (Harder, 2015). The Uinta Basin has exceeded this limit during some winters (Helmig, 2014). High ozone in the Uinta Basin has been shown to be related to emissions of methane and NMHC from the oil and gas industry (Edwards, 2013).

CHAPTER 2

BACKGROUND

2.1 Geologic Setting

The Uinta Basin is located in northeastern Utah and encompasses an area of more than 9,300 square miles (Morgan, 1999). The Uinta Basin is geographically bound on the south by the Book Cliffs, on the west by the Wasatch Mountains, on the north by the Uinta Mountains, and on the east by the Douglas Creek arch (Chapman, 1984). For this study measurements were collected in the Red Wash, Natural Buttes, and White River Fields in the Uinta Basin. The Uinta Basin is rich in hydrocarbon deposits (Anders, 1992) associated with the Cretaceous Mancos Shale and Mesaverde Group, Eocene Wasatch Formation, and the Eocene Green River Formation (Hettinger and Kirschbaum, 2002). Within these formations, the Uinta Basin contains abundant fossil fuel resources, including oil, natural gas, coal, gilsonite, tar sands, and oil shale (Anders, 1992).

Clay Basin is near the Utah-Wyoming border in northeastern Utah. The Clay Basin Field is a doubly plunging anticline that encompasses an area of 7.3 square miles (Q.P.C.). The Cretaceous Frontier and Dakota Formation are hydrocarbon reservoirs for oil and gas production. The Dakota Formation is also an underground storage reservoir for natural gas in the Clay Basin Field (Q.P.C.).

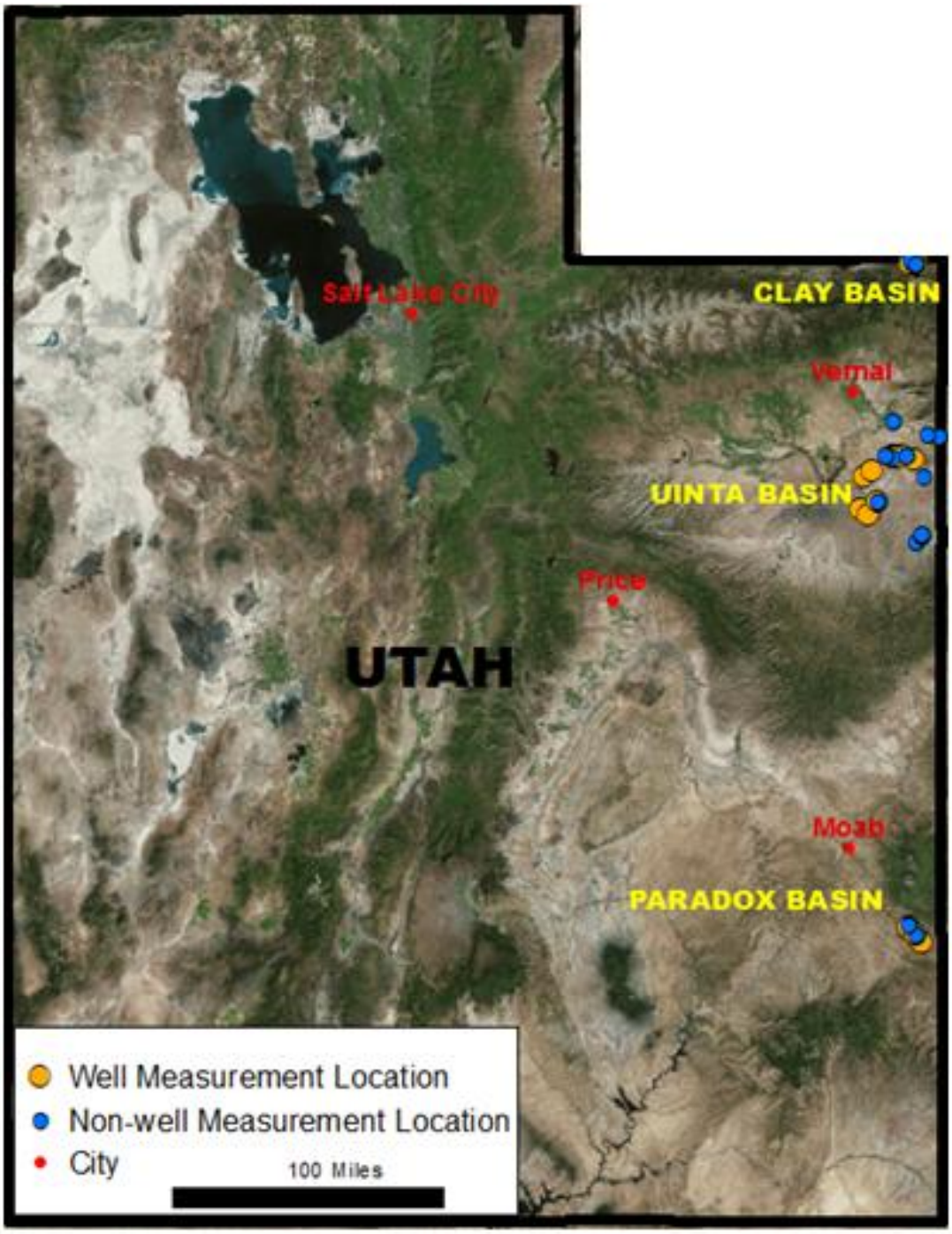

Figure 1. Map of the study area and sample locations.

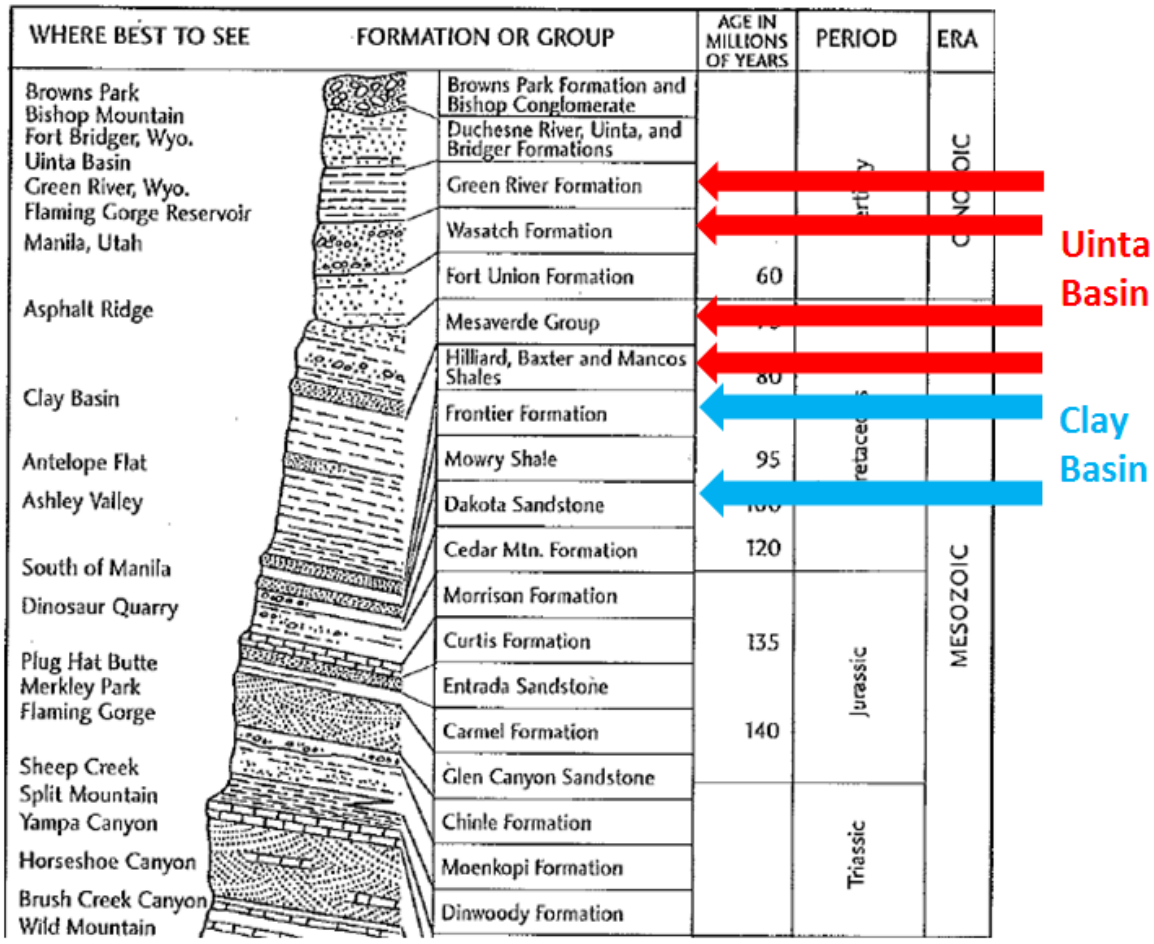

Figure 2. Stratigraphic column of Uinta and Clay Basin hydrocarbon reservoirs defined (Hansen, 2005).

The Paradox Basin is an asymmetric foreland basin located in southeastern Utah that encompasses an area of approximately 19,440 square miles (Barbeau, 2003). The Paradox Basin is geographically bound on the south by the northeast trending Hogback monocline, on the north by the Uinta Basin, on the west by the San Rafael Swell, and on the east by the San Juan dome (Nuccio and Condon, 1996). Geologic structures within the Paradox Basin consist of anticlines and scattered Tertiary laccoliths (Hanshaw and Hill, 1969) that can influence the petroleum system. The South Pine Ridge and Big Indian South Fields are located in the northcentral area of the Paradox Basin, south of Moab, UT.

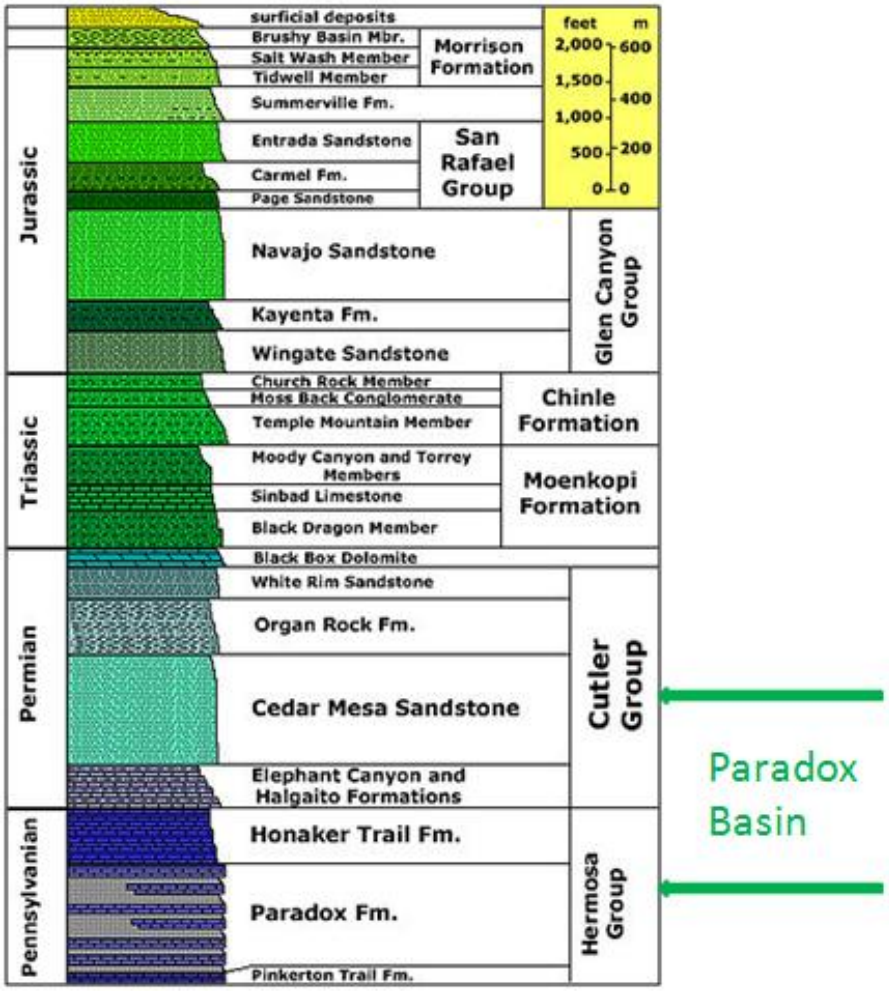

Figure 3. A Stratigraphic column of Paradox Basin hydrocarbon reservoirs defined (Baars, 2000).

2.2 Hydrocarbons and Their Potential Occurrence

When plant and animal remnants in sediment undergo burial diagenesis, the process results in organic solid hydrocarbon compounds called kerogen or coal (Selley, 1997). Kerogen and coal can be transformed into oil and gas once buried at sufficient depths and temperatures. When this occurs, kerogen and coal are thermally decomposed to form oil and gas (Rice, 1992). To generate and retain oil and gas; a petroleum system must contain organic-rich source rock, adequate conditions for thermal maturation, and a

reservoir with a trap or seal are required (Selley, 1997). The petroleum systems in the Uinta, Clay, and Paradox Basins meet all of these conditions.

Reservoirs for oil and natural gas in the Uinta Basin are in two major depositional sequences. Nearshore marine to a fluvial environment comprised the older sequence, the Upper Cretaceous Mesaverde Group. Source rocks for these hydrocarbons contain oxygen-rich organic matter, which is considered a type II kerogen that primarily produces methane gas (Tissot, 1978). The second major sequence containing reservoirs is a series of Tertiary deposits comprised of the Paleocene and Eocene North Horn, Wasatch, Colton and Green River Formations (Fouch, 1975). The most abundant source rocks in the Tertiary are the Green River Formation oil shales. The dominant oil producing beds are in the lower and middle of the Green River Formation (Morgan, 1999).

The Cretaceous Frontier Formation is the major reservoir for oil and gas production in the Clay Basin. The Frontier is variegated sandstone, interbedded with thin coal seams and shale (Walton, 1944). The highly porous and permeable Cretaceous Dakota Formation is also an oil and gas reservoir but is now primarily used for underground natural gas storage in Clay Basin. The Dakota sandstone is partly cross-bedded and comprised of conglomerate to fine grain sands interbedded with shale (Walton, 1944).

The Ismay-Desert Creek and Cane Creek Cycle intervals of the Middle Pennsylvanian Paradox Formation are the oxygen-rich source rocks, generating kerogen types I, II, and III in the Paradox Basin (Nuccio and Condon, 1996). Hydrocarbon reservoirs consist of Permian Cutler Group and the Pennsylvanian Hermosa Group. The Cutler Group is undivided and comprised of a heterogeneous sequence of conglomerates,

sandstone, siltstone, and mudstone (Condon and Huffman, 1997). The Hermosa Group contains the Desert Creek and Ismay sequences that underlie the Honaker Trail Formation. The Honaker Trail is a hydrocarbon reservoir comprised of cyclically bedded limestone, sandstone, and shale (Ritter, 2002).

Gilsonite, a solid hydrocarbon ore, has been mined in the Uinta Basin (Monson and Parnell, 1992). The veins in the Uinta Basin cut through parts of the Wasatch, Green River, Uinta, and Duchesne River Formations (Monson and Parnell, 1992).

The Eocene Green River Formation contains oil shale found predominantly in the Mahogany zone (Birdwell, 2015). Oil shale is a fine-grained rock that contains an abundant amount of kerogen (Sweeney, 1987), but has not matured to the point of liquid or gas hydrocarbon production. The United States Geological Survey (USGS) has estimated oil shale deposits of 2.845 trillion barrels of oil-in-place in Utah (Birdwell, 2015). Although the rock must be heated to 350-500°C to obtain a rapid, industrial conversion of kerogen to petroleum, lower temperatures can also convert kerogen to petroleum over time via a process known as catagenesis. Hydrocarbons can be released over time by catagenesis and escape the sedimentary rock (Birdwell, 2015) into the atmosphere. Direct measurements of methane emissions from natural geologic surfaces needs more accurate quantification (Etiope and Klusman, 2002), such as those fluxes from natural oil shale and gilsonite outcrops.

The Upper Cretaceous Blackhawk Formation contains coal seams that outcrop in the Uinta Basin. Coal is a sedimentary rock that formed along paleo-rivers and streams near sea-level in freshwater swamps. The abundance of vegetation and organic matter decaying in the swamps caused the oxygen to be used up in the decaying process and

prevented the vegetation and organic matter to decompose (Dubiel, 2000). Sediment covered the vegetation and organic matter in the swamp and preserved as peat. Coal formed from the pressure of overlying strata. During coalification methane gas and coal are formed together by biological and geological processes (Warmuzinski, 2008).

2.3 Emissions to the Atmosphere from Oil and Gas Exploration and Production

CO_2, methane and NMHC are emitted into the atmosphere from oil and gas-bearing formations, especially from those with active oil and gas production (Allen, 2013; Helmig, 2014). The U.S. Government Accountability Office (GAO) suggests that venting and flaring throughout the lifetime production of a well comprises of 0.3% to 1.9% of natural gas production loss (GAO, 2010). The National Oceanic and Atmospheric Administration (NOAA) used aircraft-based methane measurements to determine emissions of methane from the entire Uinta Basin during the winter of 2012. Atmospheric modeling coupled with aircraft measurements indicated 9% of total natural gas production was lost into the atmosphere (Karion, 2013); much higher than the GAO estimate. This discrepancy is likely due to leaks and other emission sources that are unaccounted for by the GAO.

One of the primary mechanisms for hydrocarbon leakage from a well is through valves and fittings. A completed well contains between 55 and 150 fittings and connections (Howarth, 2011). A number of studies have quantified emissions from valves and fittings on oil and gas equipment above the soil surface (e.g., Allen, 2013; Sandberg, 1989). Few measurements of emissions from subsurface natural gas infrastructure have been collected; however others have measured these sources (Day, 2014; Kang, 2014). For this study, flux measurements were collected with a DFC. DFCs are useful for direct

measurement of emissions between soil surfaces and the atmosphere (Picard, 2001). Studies by Day (2014) and Kang (2014) used the DFC for direct measurements of methane at oil and gas well sites. A study by Day (2014) in Australia used three methods; plume traverse, leak and vent testing, and surface emissions to detect leaks and measure emissions. Measurements were collected from venting, equipment, and well casing leaks from oil and gas infrastructure. DFC measurements near the wellhead did not detect any leaks. Overall, methane leaks detected were from engines used to dewater pumps, vents, pneumatic devices, and equipment leaks. A study by Kang (2014) measured emissions at abandoned oil and gas wells in Pennsylvania. DFC and carbon stable isotopes were used to identify emission sources. Wells that emitted $>10^3$ mg h^{-1} were likely derived from a thermogenic source. The abandoned wells measured were averaged, then estimated to contribute 0.3-0.5% of the methane emissions in Pennsylvania. These studies have indicated that subsurface wellbore leaks are not a significant source of methane emissions, but emissions from wellbores can be a significant source in some cases (Conley, 2016).

Multiple steps are taken to drill and complete a well. A failure at any step could lead to hydrocarbon leakage out of the well (Davies, 2014). Well casing (surface, intermediate and production) is inserted into drilled boreholes to prevent contamination of groundwater and water encroachment and to increase the structural integrity of the borehole (Downey, 2009; King and King, 2013). Well casing that was not properly sealed or damaged can provide a migration pathway for hydrocarbons (Day, 2014). Cement is pumped between the casing and the wellbore wall to seal the well and prevent leaks. A study by Jackson and Dusseault (2014) in Canada suggested that well leaks were derived

from cement shrinkage that reduces the contact stress between the cement and the wellbore wall, allowing gas to migrate towards the surface. Gaps in the cement or poorly sealed joints in casing pipe could become a migration pathway for CO_2 and hydrocarbons to escape to the atmosphere (Duguid, 2001).

Underground oil and natural gas reservoirs are sealed or trapped by overlying rock that prevents their contents from migrating upward. However, these capping formations are imperfect. One study suggests that geologic formations in Utah have been leaking natural gas since the early Tertiary (Johnson and Roberts, 2003). Natural methane seepage estimates are not well constrained because the seepage is temporally and spatially variable (Mansfield, 2014). Fault or shear zones can provide preferential pathways for seepage from subsurface hydrocarbon reservoirs when the trap is insufficient to prevent vertical hydrocarbon migration (Selley, 1997). Production of oil and gas can reduce formation pressure and cause the seepage to slow down and ultimately stop in some cases (Mansfield, 2014), whereas pressurizing a reservoir through injection of water, or natural gas for storage or CO_2 enhanced for recovery can enhance seepage (Horvitz, 1985). Etiope and Klusman (2002) used global estimates from previous studies to calculate a global microseepage flux >7 Mt y^{-1} (Megaton/year). Mansfield (2014) used the chemical composition of oil and gas source rocks to estimate hydrocarbon seepage from petroleum reservoirs in the Uinta Basin. An estimated 2900 t y^{-1} was calculated for emissions from subsurface natural gas leaks.

CHAPTER 3

METHODS

3.1 Study Locations

Three oil and gas-bearing basins in Utah were sampled for emissions from soils at well and non-well sites (Figure 1). In the Uinta Basin, thirteen wells were sampled among the Natural Buttes, Red Wash, and White River Fields. Nine wells were sampled in the Clay Basin Field. In the Paradox Basin, five wells were sampled among the Big Indian South and South Pine Ridge Fields. The wells were selected based on total combustible soil gas concentrations collected in previous years by the USGS to obtain measurements from wells with low, medium, and high total combustible soil gas concentrations. Non-well sites measured included soils within the Natural Buttes, Red Wash, Clay Basin, and South Pine Ridge Fields. In summer 2015 non-well measurement sites also included coal, gilsonite, oil shale, and a fault zone. Figure 1 shows the geographic locations of the wells and non-well sites. Wells sampled included producing, shut-in, and gas storage wells. The study included a total of 233 soil emissions measurements, including 195 well site measurements and 38 non-well measurements.

Between two and eight measurements were collected from each well pad or other measurement site during each site visit. Each measurement location on a well pad was recorded with its associated distance and direction from the wellhead and latitude and longitude were recorded for non-well sites. Each flux measurement was collected for at least 30 minutes, and average results over the collection period were used in this study.

The DFC distances from the wellhead varied between 0.3 and 5.2 meters. Measurements were commonly (17%) collected 0.6 meters away from the wellhead. The majority (93%) of the measurements were within 3.1 meters of the wellhead.

3.2 Dynamic Flux Chamber

The DFC was attached to a stainless steel collar (Figure 4), which was pressed into the ground to create a seal. The DFC was placed on the collar and clamps were used to secure the chamber to the collar (Eklund, 1992). The DFC was placed directly on the snow during winter of 2016 with the steel collar submerged in the snow. Stainless steel collars were 40 centimeter (cm) in diameter, 10 cm in height, and had a 1.5 cm edge.

The DFC was a polycarbonate half-sphere with an open-bottom. Following (Eklund, 1992), it had a 40 cm base diameter, was 20 cm in height, and had a 1.5 cm edge to clamp to the steel collar (Figure 5). The DFC had a fan attached at the top which rotated at about 100 rotations min^{-1} to create homogeneous conditions inside the chamber. Two 0.6 cm OD Teflon tubes were used to secure a pneumatic connection to the DFC and transport air from the chamber to a Los Gatos Research (LGR) Ultra-Portable Greenhouse Gas Analyzer that analyzed methane and CO_2. Canisters were analyzed for NMHC. One tube sampled air immediately from outside the chamber, whereas the other sampled air from inside the chamber with 47 millimeter (mm) Teflon filters installed near the DFC on each tube to prohibit dust from entering the tubes, which were changed periodically.

The following equation was used to calculate flux:

$$flux = \frac{(Concentrationinside - Concentrationoutside)}{Surfacearea} xFlowRate \quad (1)$$

where flux is in units of (mg m^{-2} h^{-1}), the concentration was measured in mg/m^3, the surface area was 0.13 m^2 (base area of the stainless steel collar and DFC), and the flow rate was 10 liters (L) min^{-1}.

Periodically, blank samples were measured by placing a Teflon sheet at the base of the DFC. After each measurement campaign, the chamber and tubing were cleaned with soap, ultrapure water, and methanol.

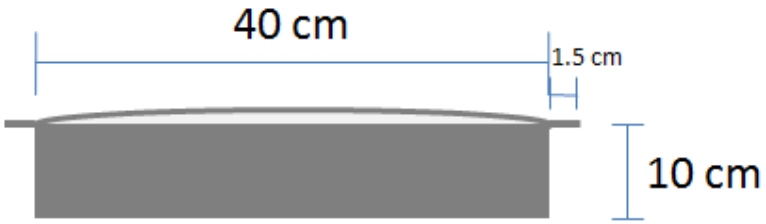

Figure 4. Steel collar dimensions.

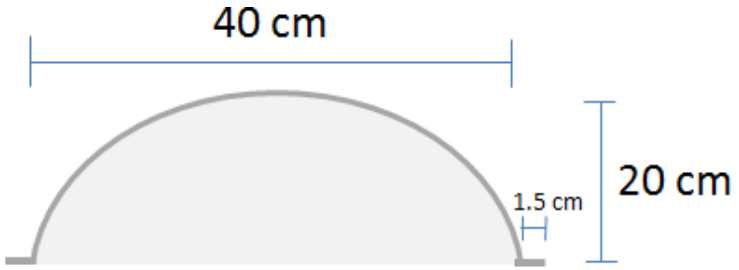

Figure 5. Cross-section of dynamic flux chamber dimensions.

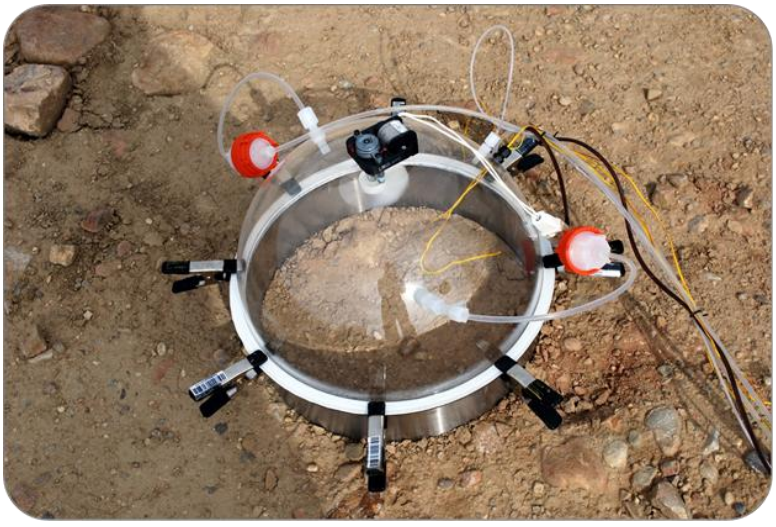

Figure 6. A picture of DFC, steel collar, and sampling equipment used to measure emissions.

3.3 Methane and CO_2 Measurements

An LGR Ultra-Portable Greenhouse Gas Analyzer was used to measure methane and CO_2 concentrations inside and outside the chamber. Using three times the standard deviation of the instrument response when subject to scrubbed air, the detection limits were ± 0.06 mg m^{-2} h^{-1} for methane and ± 18.9 mg m^{-2} h^{-1} for CO_2 fluxes. The LGR analyzer was calibrated daily using certified methane and CO_2 calibration gas with three calibrations points. A zero calibration check was accepted when CO_2 was less than 5 ppm, and methane was less than 0.025 ppm. The span calibration check was accepted when CO_2 and methane were within 5% of expected values. Calibration recovery was 98% ± 0.01% for methane (mean ± 95% confidence interval) and 98% ± 0.02% for CO_2 (mean ± 95% confidence interval).

An LGR Multiport Inlet Unit allowed the LGR analyzer to sequentially sample from inside and outside the DFC in 120-second (s) intervals. Methane and CO_2 concentration, chamber flow, and other variables were recorded in 20 or 30 s intervals using a Campbell Scientific CR1000 data logger.

3.4 Ancillary Measurements

Meteorological data, including temperature (Campbell CS215), relative humidity (Campbell CS215), barometric pressure (Campbell CS100), wind speed and direction (New Mountain NM150WX), soil temperature and moisture (0-12 cm depth, Campbell CS655) and total incoming solar radiation (Campbell CS300) were measured 6 meters above ground level. The temperatures of air and surface soil inside and outside the chamber were measured with type-k thermocouples.

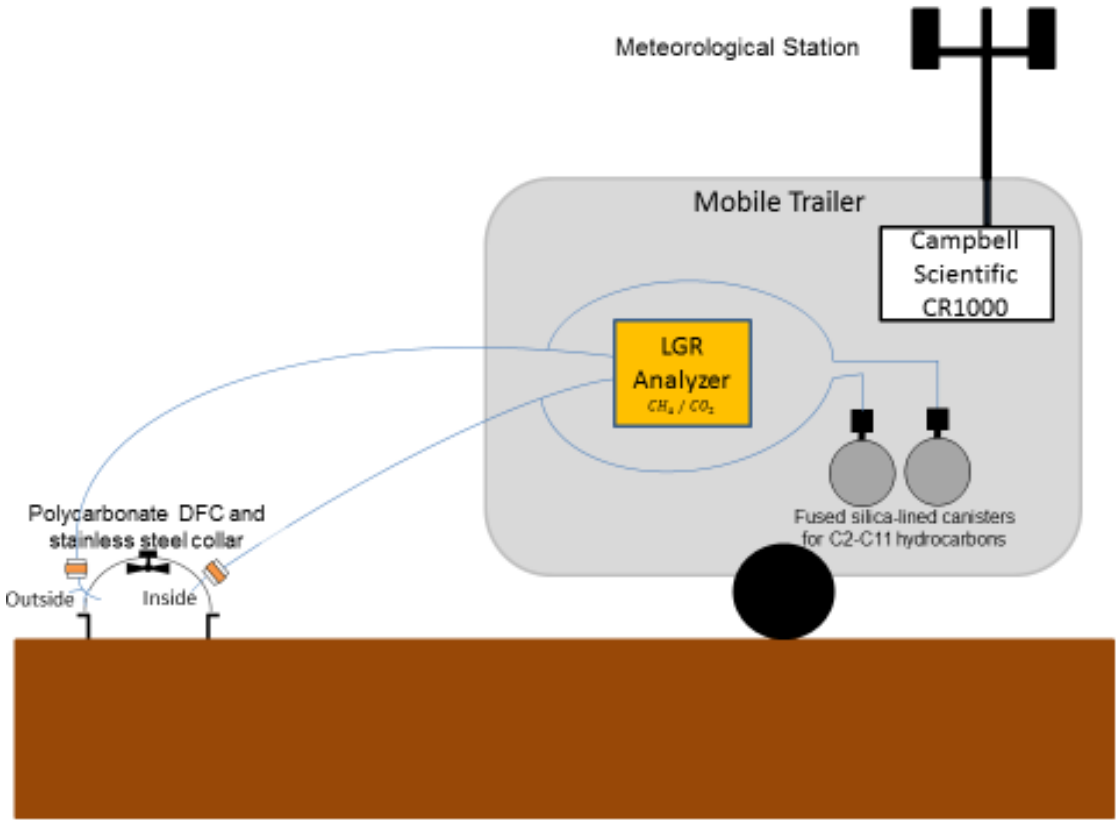

Figure 7. Set up for measuring soil emissions and meteorological data.

Evacuated, silonite coated, stainless steel 6 L canisters were filled with air from inside and outside of the chamber for some of the measurements. Mass flow controllers were used to maintain a constant flow rate during each measurement. After collection, the air inside the canisters was analyzed in the laboratory (see below). Figure 7 shows how emissions data were collected and recorded in the field.

3.5 Soil Sample Collection and Soil Gas Measurements

Soil samples were collected from each site visited in 2015. A shovel was used to dig out soil to a depth of 15 cm, and the soil was transferred to a plastic bag and sealed. Soil samples were then analyzed in the laboratory for texture (i.e., the amount of sand, silt, and clay), pH, conductivity (a proxy for the amount of salts in the soil), and total organic carbon (TOC).

Measurements of the amount of total combustible gas in soil interstitial space were collected from temporary total combustible soil gas probes using a Bascom-Turner Gas-Rover model VGI-201. The Bascom-Turner Gas-Rover detects natural gas from 10 ppm (parts per million by volume) to 100% gas with a ± 2% of sample, ± 10 ppm accuracy (manufacturer specifications). This portion of the project was carried out in cooperation with the USGS. USGS installed temporary total combustible soil gas probes at most of the wells visited for this study. USGS installed probes at well sites at various distances and directions from the wellhead. Between four and twelve probes were installed at each well site, dependent on the concentration and lateral extent of soil gas. The probes consisted of PVC pipe and perforated Teflon tubing placed into the ground at a depth of 0.3 to 0.9 meters. The lowest 15 cm of the Teflon tubing was perforated, and it was closed off at the bottom. Clean sand was placed between the tubing and the outer PVC pipe. The perforated Teflon tubing had a screw-on cap that connected to the Bascom-Turner Gas-Rover via a sampling tube. The USGS collected total combustible soil gas measurements with a Bascom-Turner Gas-Explorer model EGI-201. Two measurements were recorded; the peak value and the value after 30 seconds of sampling. Figure 8 below provides an illustration of the soil gas probes. The Bascom-Turner Gas-Rover was calibrated daily using clean ambient air and 100 ppm and 100% methane certified calibration gas. DFC measurements were collected near soil gas probes when possible.

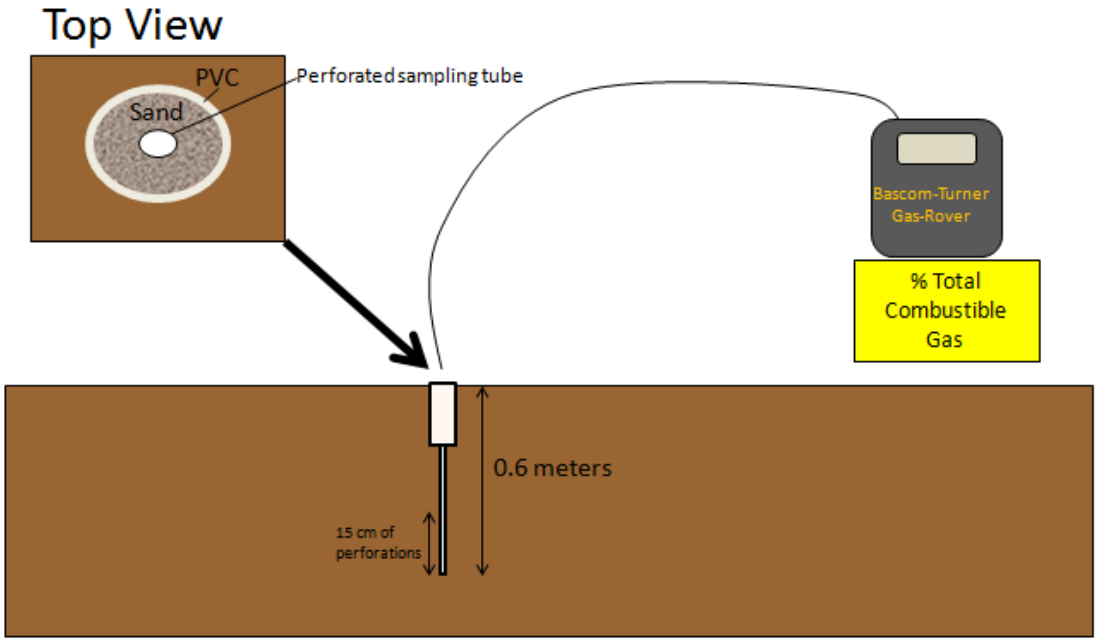

Figure 8. Illustration of total combustible soil gas probes and how total combustible soil gas measurements were collected with a Bascom-Turner Gas-Rover.

3.6 Laboratory Analysis

3.6.1 Non-Methane Hydrocarbon Analysis

Canister air samples collected from inside and outside the DFC were analyzed for C2-C11 NMHC using a derivation of the Photochemical Assessment Monitoring Stations (PAMS) method (Purdue, 1991). An Entech 7200 preconcentrator and 7016D autosampler were used to concentrate samples and introduce them to a gas chromatograph (GC) system for analysis. Cold trap dehydration was used to reduce water vapor in the sample, as described by Wang and Austin (2006).

The GC system consisted of two Shimadzu GC-2010 GCs with a flame ionization detector (FID) and a Shimadzu QP2010 Mass Spectrometer (MS). Sample introduced to the GC system first passed through a Restek rtx1-ms column (60 meter, 0.32 mm ID), and then entered a VICI four-port valve with a Valcon T rotor. For the first 5.65 min after injection, the sample then passed into a Restek Alumina BOND/Na_2SO_4 column (50 m,

0.32 mm ID) and into an FID. After 5.65 min, the valve position changed and the sample was directed into another Restek rtx1-ms column (30 m, 0.25 mm ID). Light hydrocarbons (until 2015 these included ethane, ethylene, and acetylene; after 2015, propane and propylene were also included) were quantified by FID, whereas all other compounds were quantified by MS. The temperature of the two GCs was held at 45°C for the first 15 minutes of each analysis, then increased to 170°C at a rate of 6°C per minute, and then increased to 250°C at a rate of 15°C per minute, and remained at 250°C for the last 16.8 minutes. The MS remained at a constant temperature of 200°C. The beginning of every sample batch of 15 samples consisted of a five-point calibration curve, with two calibration checks, a duplicate, and a blank check at the end of the batch. Calibration checks had an average recovery of 104.6 ± 4.1%. Duplicate samples were -0.4 ± 9.5% different. See Appendix 1 for a list of 56 NMHCs that were analyzed and quantified using the GC and MS.

3.6.2 Soil Texture

Soil samples were sieved to <2 mm grain size for soil texture characterization. 40-50 grams of each sample were then weighed and mixed with 100 mL of sodium hexametaphosphate (solid) and 200 mL of distilled deionized water. The suspension was poured into a 1000 mL hydrometer sedimentation cylinder, filling the remaining 1000mL with distilled deionized water. After the solution was mixed and sediment began to settle, temperature and hydrometer measurements were collected after 60 seconds and again after 7 hours. The mass of the soil, temperature, and hydrometer measurements were used to calculate the percent sand, silt, and clay (Soil Survey Staff, 2009). Computed soil texture of the percent sand, silt, and clay were entered into the United States Department

of Agriculture (USDA) Natural Resource Conservation Service (NCRS) Soil Texture Calculator (Soil Survey Staff, 2009).

3.6.3 Total Organic Carbon in Soil

For total organic carbon (TOC) analysis, soil samples were sieved to a 2 mm sized grains, then ground to <1 mm sized grains. Analysis was carried out with a Shimadzu TOC-VCSH Total Organic Carbon Analyzer with an SSM-5000A soil sampling module. Three-point calibrations curves were used with sucrose as the standard for total carbon (TC) and sodium carbonate as the standard for inorganic carbon (IC). The calibration curves consisted of 0, 20, and 40 mg standards. Two samples of each soil weighing 500 mg were prepared in a sample boat, one for TC, and one for IC. TOC was calculated as TC–IC=TOC. The TC sample was loaded in the SSM-5000A and analyzed first, and then the IC sample was loaded and injected with 1 mL of 25% phosphoric acid before analysis.

3.6.4 Soil pH and Conductivity

Soil pH and conductivity were measured using water extraction. 100 mg of each soil sample was sieved to a 2 mm grain size and then ground to <1 mm grain sizes. Distilled deionized water was added to the soil until it was slurry. A Mavco Extractor was used to extract liquid from the mixture, and a Vernier pH/conductivity meter measured the pH and conductivity of the extracted liquid. The pH/conductivity meter was calibrated using pH levels of 4, 7, and 10 and conductivity levels of 84, 1280, 80,000, and 111,800 millisiemens per cm (mS/cm).

3.7 Well Data

Data recorded on the Utah Division of Oil, Gas, and Mining (DOGM) website (http://oilgas.ogm.utah.gov/) were used to gather well information. Well information used included field name, well completion date, drilling history, well depth, the amount of cement, monthly and cumulative production, producing formation, well type, tubing and casing pressure, well status and chemical composition of raw natural gas. All of this information was used to correlate with methane emissions measured in this study. Tubing and casing pressures and the chemical composition of raw natural gas at most of the wells sampled were received from the BLM.

3.8 Estimated Emissions for Entire Uinta Basin

Methane emissions measured in this study were used to estimate the contribution well pad soil emissions have on the entire Uinta Basin. Averages of measurements were used to estimate the overall emissions from all well pad soils in the Uinta Basin. The average flux for a series of concentric rings around each wellhead was determined, and the sum of fluxes for all the rings was determined to be the average emission rate for each well type (producing or shut-in). The rings were delineated from 0 to 4.9 meters from the wellhead at 0.6 m intervals. The average methane flux of each concentric ring was multiplied by the concentric ring area to determine the methane flux for each concentric ring. Ring area was determined as:

$$\text{Concentric ring area } (m^2) = (\pi)\ (\text{outer radius } (m)^2 - \text{inner radius } (m)^2) \quad (2)$$

Emissions from each ring were calculated as:

$$\text{Emissions from concentric ring } (mg\ h^{-1}) = ((\text{Concentric ring area } (m^2)) \times (\text{Average flux in concentric ring } (mg\ m^{-2}\ h^{-1})) \quad (3)$$

The estimated emissions from producing and shut-in natural gas wells were extrapolated by the number of wells of each type in the entire Uinta Basin. Producing gas wells comprised of 23%, and shut-in gas wells comprised of 2% of the wells in the Uinta Basin. This estimate does not include emissions from other well types, including oil wells, and temporarily-abandoned or plugged and abandoned gas wells. Also, the wells in this study were not selected randomly, and the sample size consisted of 0.11% of wells in the Uinta Basin.

CHAPTER 4

RESULTS AND DISCUSSION

4.1 Yearly Averages

4.1.1 Non-Well Soil Surfaces

Background soil surface fluxes from 2013-2016 were comprised of 24 DFC measurements (two per sampled field per year). Table 2 shows the yearly average methane flux for each field. In this study, Natural Buttes Field averaged the highest methane flux of 0.10 mg m^{-2} h^{-1}. Natural Buttes was also the only field measured in this study with a positive flux. The difference in methane fluxes between fields was <1 mg m^{-2} h^{-1}. With only a few (<10) measurements per field, it was difficult to determine the natural emissions rate on a regional scale. Red Wash averaged the lowest methane flux of -0.9 mg m^{-2} h^{-1}.

Hydrocarbons that have migrated and accumulated at or near the surface have been found to be more concentrated in oil and gas fields (Horvitz, 1985). Concentrated hydrocarbons measured at the surface have led to the discovery of many oil and gas fields (Jones and Drozd, 1983). Natural Buttes Field was the only field that had positive average methane flux. Near zero or negative methane emissions suggests that methanotrophs consumed more methane than that produced from seepage or methanogenesis. Negative fluxes are typically measured in dry soils when methanotrophic oxidation consumes methane and produces CO_2 as a by-product (Etiope and Klusman, 2002).

In winter 2016, measurements were collected on snow covered non-well soil surfaces. When snow covers the soil surface, increased concentrations of methane and

CO_2 were found in subalpine forests in Colorado (Swanson, 2005). Methane flux decreased in winter 2016 in the Red Wash and Clay Basin Fields compare to summer 2015. A study conducted by Etiope (1999) in Italy measured the similar effect, methane flux decreased from 0.65 mg m^{-2} h^{-1} to 0.15 mg m^{-2} h^{-1} during summer and winter, respectively. The decrease in methane flux was likely caused by a reduction in biological activity when the air was consistently mixed and little or no snow was on the surface. Previous studies suggested that during colder conditions, methane bacterial decomposition decreased with temperature (Panikov and Dedysh, 2000) and methanotrophic oxidation capacity was exceeded (Klusman and Jakel, 1998).

4.1.2 Well Pad Soil Surfaces

4.1.2.1 Methane Flux

DFC measurement locations ≤1.5 meters from the wellhead comprised 63% of the measurements; an annual average of these values is shown in Table 2. Only four of 73 DFC measurements >1.5 meters away from the wellhead had methane fluxes >10 mg m^{-2} h^{-1}, and these measurements were not included in the average methane flux calculations. The DFC was not always placed in the same location each year, and this could have influenced the methane fluxes measured. Eight of the wells averaged a methane flux near background (<1 mg m^{-2} h^{-1}) levels. Seven of the wells averaged a methane flux between 1 and 10 mg m^{-2} h^{-1}. Ten of the wells averaged a high methane flux (>10 mg m^{-2} h^{-1}). Two of the wells did not have measurements within 1.5 meters of the wellhead.

Average methane emissions measured from well pad soils were higher in winter than summer (Figure 9). The average methane flux increased from 67 mg m^{-2} h^{-1} (95% confidence interval) in summer 2015 to 206 mg m^{-2} h^{-1}(95% confidence interval) in

winter 2016. Increased methane flux was likely due to the accumulation of escaped raw natural gas in the snow.

CO_2 flux was significantly correlated (R^2=0.42, p<0.01, n=195) with methane flux (Table 3). CO_2 fluxes were higher than methane fluxes 92% of the time at well sites CO_2 flux was likely higher due to the decay of leaked gas and other organic matter by bacteria (Chapman and Thurlow, 1996). The 8% of methane fluxes that exceeded those of CO_2 tended to be very high, with an average methane flux of 860 mg m^{-2} h^{-1}.

4.1.2.2 Total Combustible Soil Gas

Between 2013 and 2016, 179 total combustible soil gas measurements were collected at 21 of the 27 wells measured for soil emissions. Total combustible soil gas measurements were only collected at well sites. Appendix B1 shows a list of wells visited between 2013 and 2016 with soil gas measurements ≤1.5 meters from the wellhead. Measurements ≤1.5 meters were used because 86% of the methane fluxes at distances >1.5 meters were <1 mg m^{-2} h^{-1}. Measurements of total combustible soil gas concentrations ranged from 0 to 900,000 ppm. The amount of total combustible gas varied from year to year and well to well. The variation could be from some of the revisited wells that experienced absent or damaged soil gas probes. Between summer 2015 and winter 2016, 51% of the soil gas probes were measured in both years. Without available and consistent soil gas probes, averages may be skewed.

4.1.3 Hydrocarbon-Bearing Outcrops

In summer 2015, 14 hydrocarbon-bearing outcrops were measured for emissions in the Uinta Basin. Appendix B2 shows location coordinates and the number of measurements collected at each hydrocarbon-bearing outcrop and fault zone. The

methane fluxes from hydrocarbons-bearing outcrops were low (<1 mg m^{-2} h^{-1}) among the measurements collected for this study (Figure 10).

There are few flux measurements on inactive surface coal mines compared to underground or active coal mining sites. Coal emissions have focused on mining impact, but not on undisturbed coal outcrops. Methane emissions from coal outcrops in the Uinta Basin ranged from 0 to 0.02 mg m^{-2} h^{-1}. Natural coal-bearing outcrops have low methane emissions. Some of the coal seams have little or no methane in them. Similarly, a study by Theielemann (2000) in Germany measured methane emissions from coal outcrops that ranged from -0.01 to -0.03 mg $m^{-2}h^{-1}$.

Among hydrocarbon-bearing outcrops, gilsonite had the lowest average methane flux of -0.07 mg m^{-2} h^{-1}. Methane fluxes from hydrocarbon-bearing outcrops were similar to non-well soil emissions. The emissions from hydrocarbon-bearing outcrops were near zero and near the detection limit (± 0.06 mg m^{-2} h^{-1}), therefore, they are not a significant source of emissions.

4.1.4 Fault Zone

Fractured and faulted controlled natural gas seeps within oil and gas fields contribute to escaped hydrocarbons to the atmosphere (Ririe and Sweeney, 1993). Faults provide the best natural pathways for hydrocarbon migration (Jones and Drozd, 1983). The measurements from this study were collected from the damage zone near the Uinta Basin boundary fault. The methane flux ranged from 0.04 to 0.09 mg m^{-2} h^{-1} with an average methane flux of 0.07 mg m^{-2} h^{-1}. The fault zone had the highest average methane flux among natural geologic surfaces measured in this study. The emissions were low and similar to previous studies that measured methane fluxes from -0.25 to 0.13 mg m^{-2} h^{-1} in

Piceance, Colorado (Klusman, 2000) and -0.62 to 0.80 mg m^{-2} h^{-1} in Powder River, Wyoming (Klusman and Jakel, 1998).

Table 1. The yearly average of methane flux (mg m^{-2} h^{-1}) of non-well soils with a 90% confidence interval.

Field	Summer 2013 Average Methane Flux	Summer 2014 Average Methane Flux	Summer 2015 Average Methane Flux	Winter 2016 Average Methane Flux	Total Average Methane Flux
South Pine Ridge		-0.04 ± 0.03	-0.08 ± 0.11		-0.06 ± 0.04
Red Wash	-0.06 ± 0.08	-0.03 ±0.01	-0.06 ± 0.22	-0.20 ± 0.15	-0.09 ± 0.05
Natural Buttes			-0.06 ± 0.24	0.26 ± 0.72	0.10 ± 0.24
Clay Basin	-0.15 ± 0.13	-0.05 ± 0.02	0.01 ± 0.01	-0.08 ± 0.23	-0.07 ± 0.04

Table 2. Annual and total average methane fluxes (mg m^{-2} h^{-1}) of each well with a 90% confidence interval. Average methane fluxes for each well were calculated for measurements within 1.5 meters from the wellhead. Wells with no displayed 90% confidence interval had only one measurement collected.

Field Name	Well Name	Summer 2013 Average Methane Flux	Summer 2014 Average Methane Flux	Summer 2015 Average Methane Flux	Winter 2016 Average Methane Flux	Total Average Methane Flux
SOUTH PINE RIDGE	MIDDLE MESA FED 25-41-29-24			1.2 ± 1.6		1.2 ± 1.6
SOUTH PINE RIDGE	MIDDLE MESA FED 31-31-29-25			2.2 ± 1.2		2.2 ± 1.2
SOUTH PINE RIDGE	MIDDLE MESA FED 4-20-30-25		N/A			N./A
BIG INDIAN SOUTH	BULL HORN FED 15-14-30-25		0.2 ± 0.5	0.1 ± 0.4		0.2 ± 0.2
BIG INDIAN SOUTH	BULL HORN FED 9-14-30-25		1.3 ± 10.7			1.3 ± 10.7
RED WASH	RW 34-22C	71.7		496.2 ± 3147.9	1759.1 ± 9422.0	916.5 ± 1300.1
RED WASH	RW 32-22B	61.8 ± 386.9	15.5 ± 97.9	-0.1 ± 0.8	-0.8 ± 2.3	16.9 ± 25.5
RED WASH	RW 21-22B	3.3	13.8 ± 62.7	0.6	2.8	6.8 ± 9.1
RED WASH	RW 5C1-23B		1.1 ± 7.1	0.2 ± 0.6	32.4 ± 203.2	11.2 ± 21.5
RED WASH	RW 12B1-23B		0 ± 0.1	0 ± 0.5	-0.8 ± 5.6	-0.3 ± 0.6
RED WASH	RW 21-19C		N/A			N./A
RED WASH	RW 22-22B	0.2				0.2
NATURAL BUTTES	CWU 1362-25			54.6 ± 109.4	71.5 ± 67.0	63.0 ± 54.7
NATURAL BUTTES	NBU 1022-9K-2T			0 ± 0.1	-0.2 ± 2.3	-0.1 ± 0.9
NATURAL BUTTES	NBU 141			0.9	-2.2	-0.7 ± 9.8
NATURAL BUTTES	UTE TRAIL U 83X9H			0.2	0.9	0.6 ± 2.3
NATURAL BUTTES	OU GB 3W-20-8-22			5.0 ± 10.6	373.0 ± 556.6	189.0 ± 245.8
WHITE RIVER	GB 11ML-10-8-22			0.2 ± 0.5	11.6 ± 30.8	5.9 ± 10.8
CLAY BASIN	CLAY BASIN UNIT 12	3427.0 ± 21624.1	13.4 ± 59.3	2.3 ± 2.6	36.4 ± 11.0	699.7 ± 1253.1
CLAY BASIN	CLAY BASIN UNIT 7			2.8 ± 8.2	1099.9 ± 1286.3	551.4 ± 770.6
CLAY BASIN	CLAY BASIN UNIT 54-S		0.1	12.6 ± 79.4	0 ± 0.3	5.1 ± 10.7
CLAY BASIN	CLAY BASIN UNIT 2		0.9 ± 6.8	826.0 ± 2409.5	867.0 ± 2276.1	635.1 ± 751.3
CLAY BASIN	CLAY BASIN UNIT 19	1285.7 ± 8117.4		4.8 ± 31.4	98.4 ± 410.2	462.9 ± 851.3
CLAY BASIN	CLAY BASIN 24-S		0 ± 0.1			0 ± 0.1
CLAY BASIN	CLAY BASIN UNIT 23	1.0 ± 5.4				1.0 ± 5.4
CLAY BASIN	CLAY BASIN UNIT 61	-1.1				-1.1
CLAY BASIN	CLAY BASIN UNIT 18	14.0				14.0

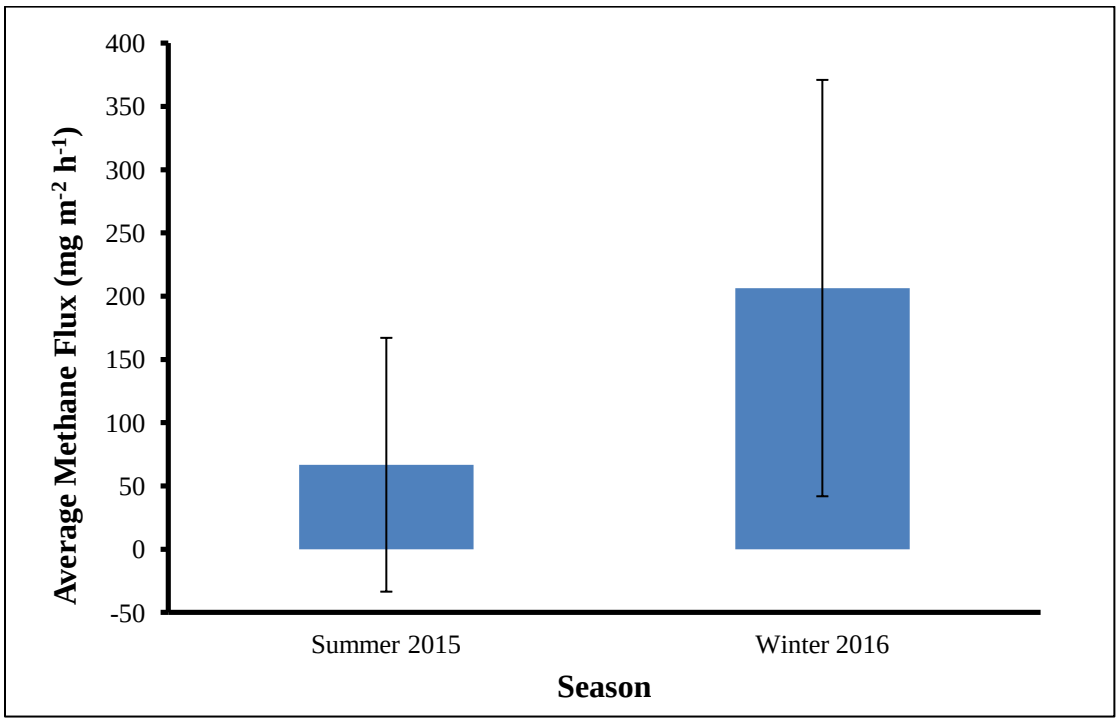

Figure 9. The average methane flux of well pad soils in summer 2015 and winter 2016. Whiskers represent a 95% confidence interval.

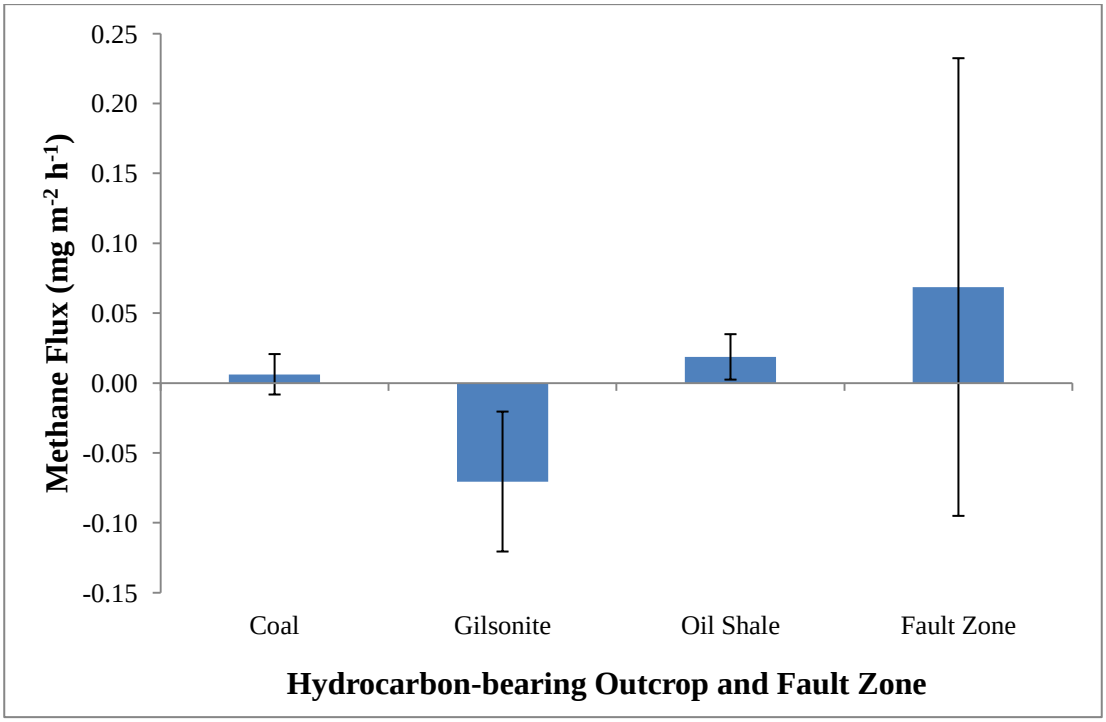

Figure 10. 2015 average methane flux of hydrocarbon-bearing outcrops. Whiskers represent a 90% confidence interval.

4.2 Oil and Gas Fields

4.2.1 Comparison Among Fields

Figure 11 shows methane and CO_2 flux and combustible soil gas concentrations for each field. Clay Basin had the highest average methane flux of 176 mg m^{-2} h^{-1} and highest average total combustible soil gas of 161,000 ppm. Big Indian South Field had the lowest average methane flux of 0.5 mg m^{-2} h^{-1}. Red Wash Field had the lowest total combustible soil gas with an average of 47,000 ppm. The relationship between methane flux and total combustible soil gas was not consistent among fields.

4.2.2 Hydrocarbon Composition

The hydrocarbon chemical compositions of emissions were variable between fields. Figure 12 shows hydrocarbon flux organized by methane, alkanes (C2-C11), alkenes, and aromatics in each field. Methane emissions dominated Big Indian South, Red Wash, Natural Buttes, White River and Clay Basin Fields. When methane concentrations were greater than NMHC concentrations, the emissions source was likely from a leaking well. All of the fields had an average methane emission greater than alkanes, except for South Pine Ridge Field. Natural gas leaks have also been identified by an abundance of alkanes in an oil field (Brandt, 2014). The South Pine Ridge Field is an alkane-rich field; containing paraffin suggests that emissions are from a leaking well (Lillis, 2003).

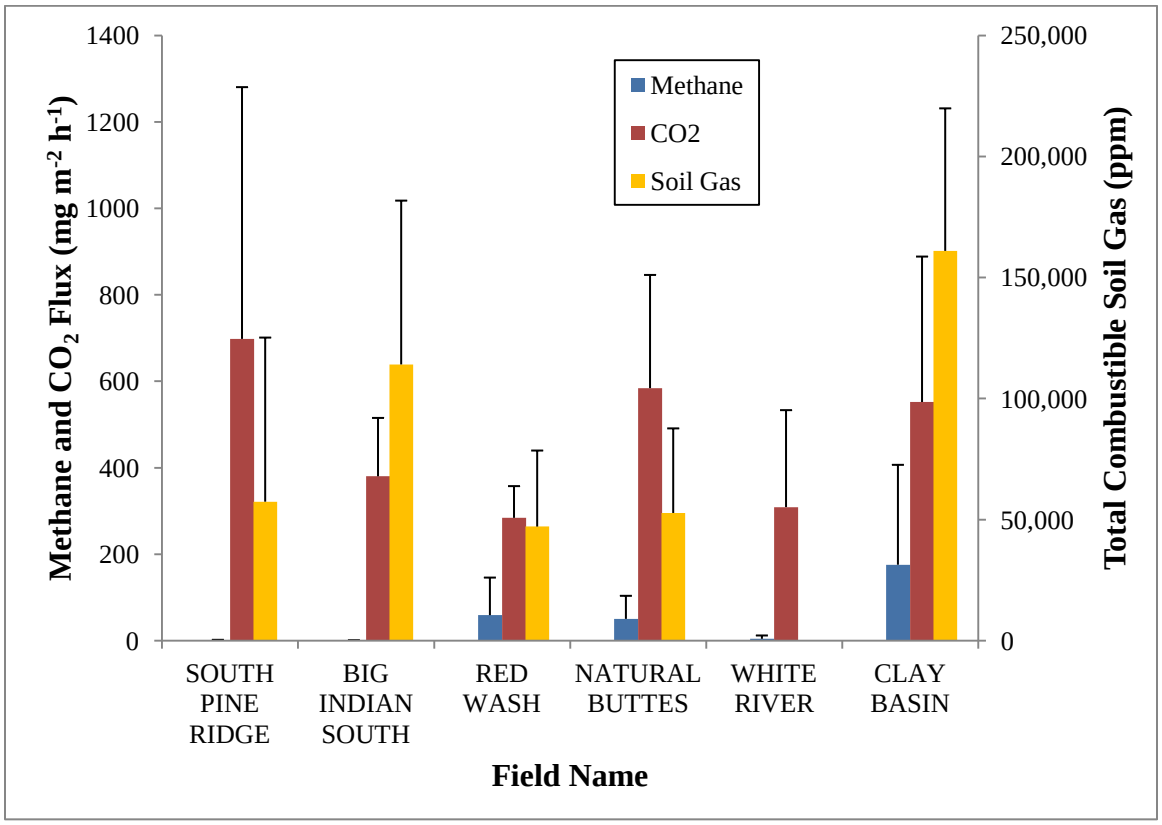

Figure 11. Field averages of methane, CO_2, and total combustible soil gas measurements collected at well sites. Whiskers indicate a 90% confidence interval.

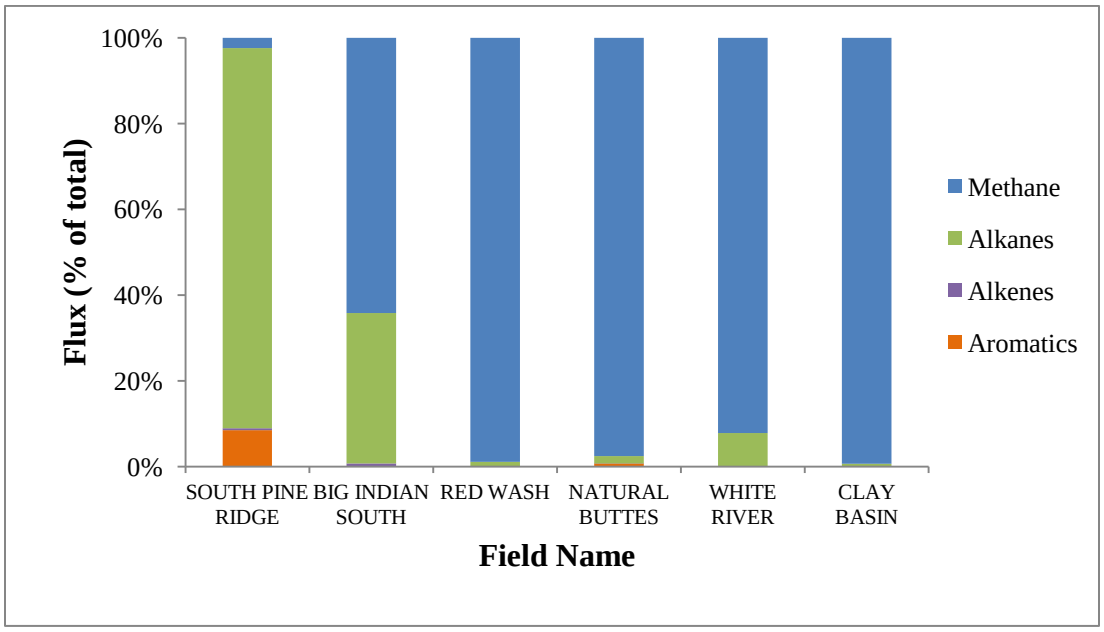

Figure 12. The relative hydrocarbon emissions composed of methane, alkanes (C2-C11), alkenes, and aromatics. The compositions as a percentage of hydrocarbon emissions from well pad soil surfaces.

4.3 Correlation of Flux with Meteorology

4.3.1 Non-Well Soil Surfaces

Overall, meteorological factors were poorly correlated with methane flux from non-well soils, well pad soils, and hydrocarbon-bearing outcrops and thus did not appear to affect non-well soil emissions (Table 3).

4.3.2 Well Pad Soils

Meteorological data and methane flux from well pad soils were also poorly correlated. Soil H_2O content was positively significantly correlated (R^2=0.55, $p<0.01$, n=148) with methane flux. The amount of moisture in the soil may have inhibited a pathway for escaped hydrocarbons by occupying the pore space, or may contribute by swelling clay particles. When soil saturation decreases, it causes an increase in emissions because of localized gas flows (Praagman and Rambags, 2008). Methane diffuses about 10,000 times faster in the air than in water (Topp and Pattey, 1997). Air filled soils are more porous than water filled soils and allow more gases to flow through the soil.

4.3.3 Hydrocarbon-Bearing Outcrops

Methane fluxes from hydrocarbon-bearing outcrops were significantly correlated with barometric pressure (R^2=0.76, $p<0.01$, n=13) (Table3). Seasonal changes in temperature and barometric pressure have been shown in other studies to influence methane emission of hydrocarbon-bearing outcrops (Kirchgessner, 2000). Barometric pressure gradients can cause an exchange of hydrocarbons in soil to the atmosphere. Barometric pumping occurs when the barometric pressure decreases, causing increased soil emissions (Xu, 2014). In this study, the opposite occurred; higher barometric pressure was associated with increased methane emissions. Multiple meteorological

conditions may be influencing the correlation between methane flux and barometric pressure.

4.4 Soil Properties

Hydrocarbon absorption likely changed soil properties and affected methane flux. During the summer of 2015, 27 soil samples were collected. Table 4 shows the linear correlations between methane flux and soil properties collected at well and non-well sites. At well sites, methane flux was correlated best with pH (R^2=0.73, p=0.01, n=7). Low pH and high methane flux were correlated, low pH inhibits hydrocarbon absorption. Dryness and salinity of the soil impact emissions at the surface (Horvitz, 1985). Acidic soils are also a factor that influences methane emissions. Acidic soils (pH as low as 3) have shown to prevent hydrocarbon absorption (Horvitz, 1985). Although measurements in this study were not acidic, the lowest pH had the highest methane flux. Methane flux and TOC were also significantly correlated (R^2=0.66, p=0.03, n=7) and is consistent with studies of methane sorption in gas shales (Chalmers and Bustin, 2008).

Four non-well site soil samples were collected near the DFC and correlated best with TOC (R^2=0.98, p=0.01, n=4). TOC was significantly correlated with methane flux because the organic carbons were measured from soil emissions and properties (Topp and Pattey, 1997). Clays are more absorptive than sand and can increase hydrocarbon accumulation (Horvitz, 1985). However, this was not reflected in these results. The percent clay did not affect methane flux in this study.

Table 3. Relationships with methane flux from non-well, well, and hydrocarbon-bearing outcrop sites. R^2 values are shown when p-values were <0.05 and were significantly correlated with methane flux. Not significant is labeled as N.S. Not applicable is labeled as N/A.

Correlation with Methane Flux	Non-well	Well	Hydrocarbon-Bearing Outcrop
	R-squared value	R-squared value	R-squared value
CO_2 Flux (mg m^{-2} h^{-1})	N.S.	0.42	0.32
In H_2O Temperature (°C)	N.S.	N.S.	N.S.
Out H_2O Temperature (°C)	N.S.	N.S.	N.S.
In Air Temperature (°C)	N.S.	N.S.	N.S.
Out Air Temperature (°C)	N.S.	N.S.	N.S.
Ambient Temperature (°C)	N.S.	N.S.	N.S.
Ambient Relative Humidity (%)	N.S.	N.S.	N.S.
Dew Point (°C)	N.S.	0.03	N.S.
Solar Radiation (W/m^2)	N.S.	N.S.	N.S.
Barometric Pressure (mbar)	N.S.	N.S.	0.76
Soil H_2O Content (m^3/m^3)	N.S.	0.55	N/A
Soil Electric Conductivity (dS/m)	0.26	N.S.	N/A
Soil Temperature (°C)	N.S.	N.S.	N/A

Table 4. Well and non-well soil properties correlated with methane flux. R^2 values are shown when p-values were <0.05 and were significantly correlated with methane flux. Not significant is labeled as N.S.

Correlation with Methane Flux	Well	Non-well
	R-squared value	R-squared value
% Total Organic Carbon	0.66	0.98
pH	0.73	N.S.
Conductivity	N.S.	N.S.
Soil Texture	N.S.	N.S.

4.5 Chemical Composition

The chemical composition of methane, NMHC, and CO_2 were also measured at the wellhead (Figure 13). The raw natural gas data reported to the BLM that was

collected from the wellhead were compared with emissions measured in this study. Figure 13 shows the composition of raw natural gas measured at the wellhead and measured well pad soil emissions. The concentration of methane, NMHC, and CO_2 measured from raw natural gas did not reflect the same composition of emissions measured from well pad soils. CO_2 comprised of less than 1% (by volume) of raw natural gas at the well sites but made up more than 70% (by volume) of the measured emissions from well pad soils. Methane made up more than 88% (by volume) of raw natural gas at the well, but only 26% (by volume) of emissions from well pad soils. Methane production can increase CO_2 flux due to the decomposition of methane by bacteria (Etiope and Klusman, 2002; Chapman and Thurlow, 1996). Methane is stable if found in closed natural gas pockets, but when in the presence of oxygen, methane is oxidized to CO_2 by the bacteria that uses the gas for carbon and energy (Etiope and Klusman, 2002; Topp and Pattey, 1997). NMHC are heavier and could be absorbed into the soil, whereas methane is lighter and can migrate toward the surface, increasing the availability of methane to be oxidized to CO_2 (Horvitz, 1985; Ririe and Sweeney, 1993).

NMHC fluxes were analyzed and compared to methane fluxes for identification of emissions sources. 68 air-filled canisters sampled were analyzed for NMHC. Methane fluxes were correlated with ethane and propane fluxes (Figure 14). Methane fluxes that correlate with propane and ethane suggest that the majority of the emissions were coming from raw gas leaks, since methane due to bacterial methanogenesis is not associated with ethane or propane (Kang, 2014), and soil emissions from liquid hydrocarbon spills would tend to contain heavier hydrocarbons (Ririe and Sweeney, 1993). The correlation of methane fluxes with ethane and propane fluxes could be due to differences in the relative

concentrations of those compounds in raw natural gas at sampled wells, or because of differing rates of methanogenesis or methanotrophy by bacteria in soils (Horvitz, 1985).

Soil surfaces can also emit hydrocarbons if contaminated with liquid hydrocarbon spills (Ririe and Sweeney, 1993). The lighter hydrocarbons are first to volatilize into the atmosphere, and ethane and propane are gases at ambient temperature, therefore emissions due to oil spills are likely to be dominated by heavier hydrocarbons. The combination of light and heavy hydrocarbons in emitted gas may indicate a combination of leaks, spills, and methanogenic processes contributed to the emissions.

NMHC concentrations can be used to estimate the amount of time the hydrocarbons had been exposed to the surface and volatilized. Ririe and Sweeney (1993), using an NMHC GC technique, identified some different classes of emission profiles based on the origin of hydrocarbons in the soil. Their technique was applied to this study to determine the source of the hydrocarbon emissions in this study. An abundance of C6 and heavier hydrocarbons in emissions was assumed to indicate emissions from liquid hydrocarbon spills (Ririe and Sweeney, 1993). When methane was higher than NMHC, the measurement was categorized as a raw gas leak.

Using this criterion, 68% of the measurements were from raw gas leaks, and 32% were from liquid hydrocarbon contamination in the soil. In all cases, when methane flux was >10 mg m^{-2} h^{-1}, methane flux was greater than NMHC flux, suggesting that large methane fluxes tend to be due to raw gas leaks. Emissions categorized as raw gas leaks had average fluxes of 312 and 4 mg m^{-2} h^{-1} for methane and NMHC, respectively, whereas emissions categorized as due to liquid hydrocarbon contamination had average fluxes of 0 and 7 mg m^{-2} h^{-1} for methane and NMHC, respectively.

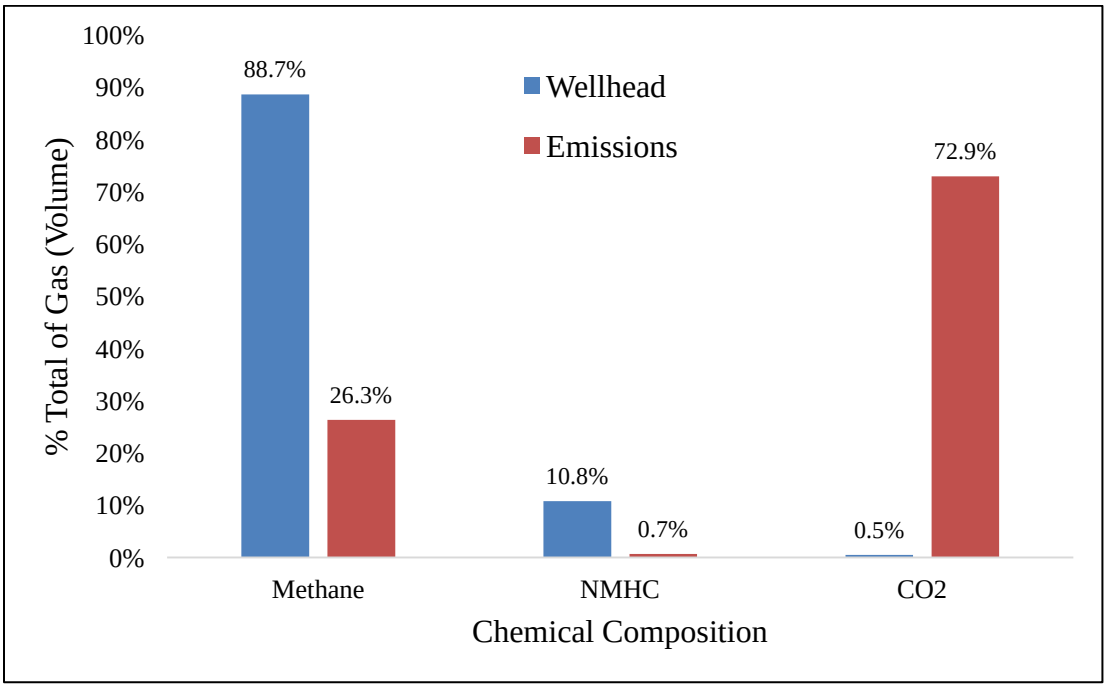

Figure 13. % Total (volume) of methane, NMHC, and CO_2 measured at the wellhead from raw natural gas and well pad soil emissions.

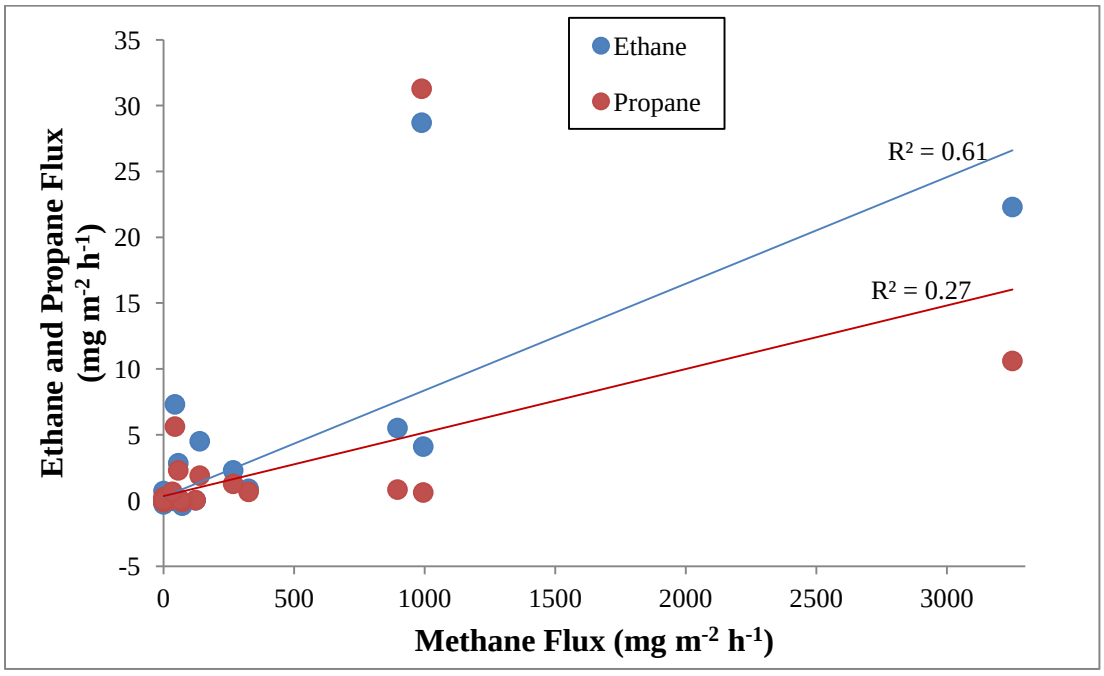

Figure 14. Ethane and propane fluxes plotted against methane flux.

4.6 Methane Flux Relationship with Total Combustible Soil Gas

4.6.1 Total Combustible Soil Gas

Methane flux and total combustible soil gas measurements were poorly correlated (R^2=0.29, p<0.01, n=63; Figure 15). The DFC was placed within 0.3 meters of soil gas probe locations when possible. Total combustible soil gas can be affected by subsurface migration pathways or covered oil contaminated soils (Ririe and Sweeney, 1993). A poor linear correlation between methane flux and total combustible soil gas was likely due to extremely localized hydrocarbon absorption and volatilization rates (Horvitz, 1985; Ririe and Sweeney, 1993). Figure 17 is an example of how hydrocarbon concentrations are spatially variable.

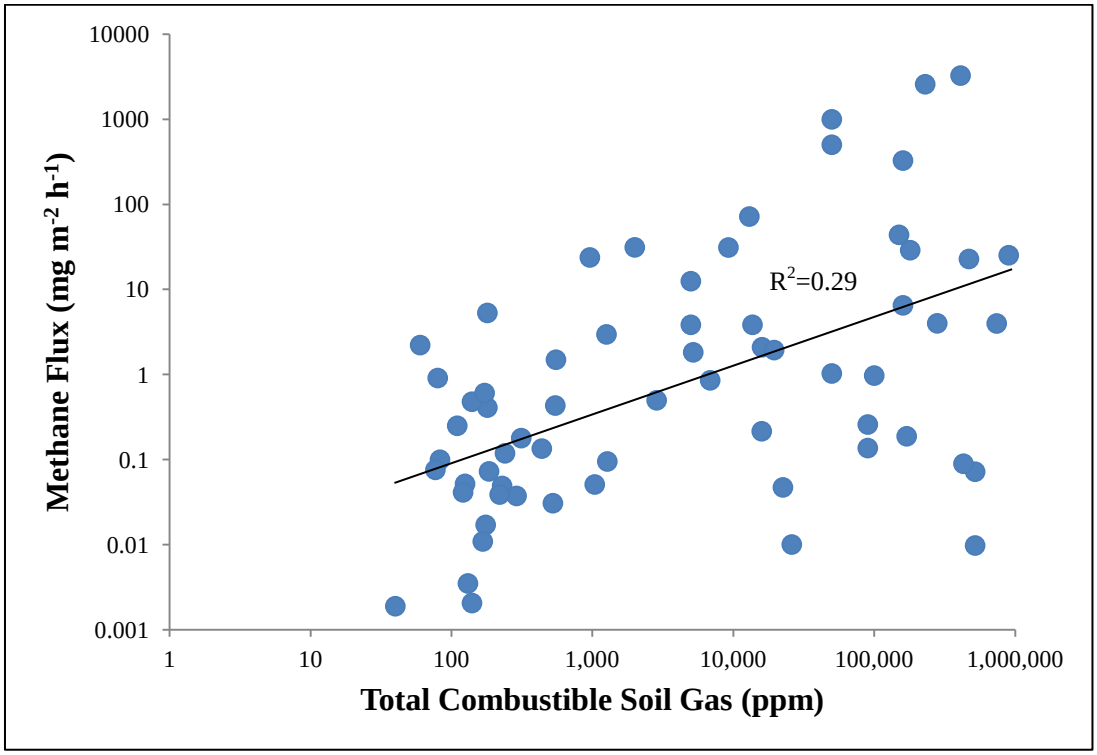

Figure 15. Methane flux and total combustible soil gas correlation on a logarithmic scale. Methane flux and total combustible soil gas with the same direction and distance from the wellhead.

4.7 Distance from the Wellhead

4.7.1 Methane Flux

Higher fluxes were often observed closer to the wellhead. In 2013, Clay Basin Unit 12 measured the highest methane flux of 6852 mg m^{-2} h^{-1}at a distance of 0.6 meters from the wellhead. In 2016, the same well measured the lowest methane flux of -5.6 mg m^{-2} h^{-1}, located 2.0 meters from the wellhead. Individual methane flux measurements and distance from the wellhead were poorly correlated (R^2=0.24, p<0.01, n=148) (Appendix C1). Averages every 0.3 meter intervals of methane fluxes improved the correlation (R^2=0.89, p<0.01, n=11; Figure 16). The average methane flux was <1mg m^{-2} h^{-1} at distances greater than 2.4 meters from the wellhead. Methane emissions were not evenly distributed around the wellhead, and high emissions were observed randomly. With only a few DFC locations around each wellhead, the point of highest emissions around the wellhead could have been missed. Based on observations, emissions on average were highest nearest the wellhead (Figure 16).

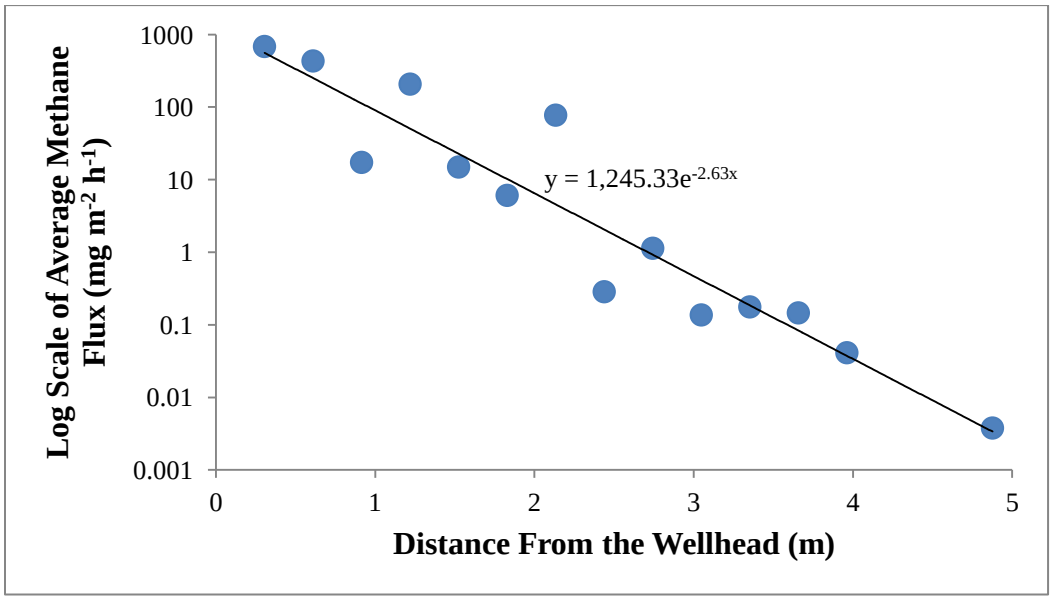

Figure 16. Average methane flux (log scale) and distance from the wellhead.

4.7.2 High-Density DFC Measurements

In spring 2016, methane and CO_2 fluxes were measured from 23 DFC measurement locations in a single day from well RW 34-22C to better understand the spatial distribution of fluxes from well pad soils (Figure 17). The well was shut-in during these measurements. DFC sample time was reduced to ten minutes. The measurements were collected at 0.6, 1.2, 1.8, and 2.4 meters from the wellhead. The lowest methane flux measured was -4.35 mg m^{-2} h^{-1}, and the highest flux was over the range of the LGR analyzer, but was estimated to be 70,000 mg m^{-2} h^{-1} (Appendix C2). Methane and CO_2 fluxes were poorly correlated (R^2=0.01, p=0.63, n=22). High methane flux of 3,500 ± 6,282 mg m^{-2} h^{-1} (95% confidence interval) and low NMHC flux of 39 ± 90mg m^{-2} h^{-1} (95% confidence interval) showed that raw natural gas leakage was the likely emissions source.

Measurements from four DFC locations around this well in January 2016 resulted in a methane flux of 886 ± 2,515mg m^{-2} h^{-1} (95% confidence interval). In April 2016 an average methane flux of 3,500 ± 6,282 mg m^{-2} h^{-1} (95% confidence interval) was measured for the 23 locations sampled in spring 2016. The results from January and April were not significantly different (p=0.41).

The high-density DFC measurements from the shut-in well showed intermittent leaks. Standing rain water was present when the well was sampled, and bubbles were visible coming from the soil. Intermittent gas migration has shown to attribute to the effect referred to as ‘Taylor bubbles’ (Jackson and Dusseault, 2014). Taylor bubbling occurs when natural gas rises through fissures in the rock as gas slugs in a pulsed flow. Taylor bubbling also occurs when the wellbore undergoes a perforation-and-cement-

squeeze process, producing narrow non-uniform gaps in the cement around the casing. The result would be intermittent and asymmetric leaks around the wellhead (Jackson and Dusseault, 2014). These high density measurements, as well as the occurrence of bubbling, indicated that methane emissions at this well were more dependent on direction from the wellhead than distance likely caused from soil or bedrock heterogeneity.

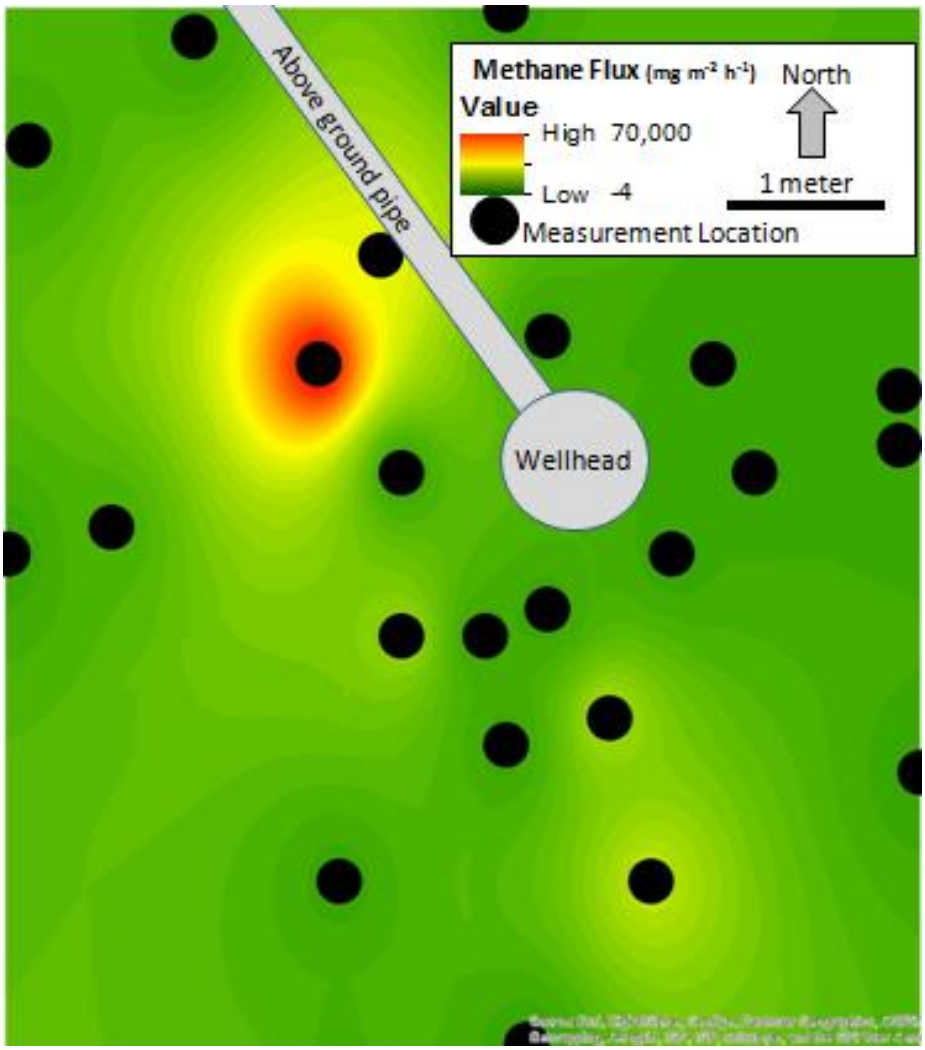

Figure 17. Methane fluxes from 23 DFC locations at well 34-22C. Background color indicates measured methane flux, and was interpolated by Inverse Distance Weighted (IDW) in ArcGIS.

4.7.3 Total Combustible Soil Gas

The individual soil gas concentration and distances from the wellhead were poorly correlated (R^2=0.07, p<0.01, n=176). Soil gas concentration averages were calculated every 0.3 meters from the wellhead. When average soil gas concentration were applied, the correlation improved (R^2=0.48, p<0.01, n=15). The highest average (263,612 ppm) total combustible soil gas was measured 0.6 meters from the wellhead. Soil gas concentrations increase when hydrocarbons are sorbed to the soil (Ririe and Sweeney, 1993). Areas closer to the wellhead would likely have more hydrocarbon sorption if leaks occur near the drilled hole.

4.8 Well Properties

4.8.1 Methane Flux Correlation

Well properties were poorly correlated with the average methane flux of each well, including casing and tubing pressure, number of days to complete drill hole, total depth of the well, daily and cumulative natural gas production, the number and feet of perforations, the number of cement sacks, the number and depth of surface cement sacks. The tubing pressure had the best correlation, but was still poor. All of the well property correlations were $R^2 \leq 0.15$.

4.8.2 Well Age

The year of well completion ranged from 1935 to 2013. The age of each well was poorly correlated with methane flux (R^2=0.12, p=0.08, n=27) and total combustible soil gas (R^2=0.10, p=0.21, n=18). Figure 18 shows the correlations between average methane flux and decade age intervals (R^2=0.49, p=0.03, n=9). Davies (2014) suggested that corrosion of steel casing and cement weakness can decrease the well integrity. The longer

the wellbore has been in the subsurface, the more corrosion and deterioration occurs, and the more likely the wellbore is to fail. Regulations regarding well control (blowout prevention equipment) and casing program (cementing casing methods) have been enforced to decrease equipment leaks (Utah Dept. of Administrative Services, 2016). A study by King and King (2013) suggests that there are multiple factors that change the rate of well integrity, but the last 15 years have brought the best improvements in well-construction and design.

4.8.3 Well Status

Figure 19 shows the average methane flux for wells that were producing, shut-in, or used for natural gas storage. Producing wells had the least variability in methane flux. Shut-in wells were the most variable. Shut-in wells have higher pressure than producing wells (DEEDI, 2010) and can increase the leak rate of the well (Day, 2014). Increased pressure in shut-in wells could lead to increased leak rates from existing leak pathways. Methane fluxes were poorly correlated with well pressure in this study, possibly because leaks were not uniformly present in wells, so the effect of pressure on leak rates was not consistent.

4.8.3.1 Methane Emissions Estimate for Uinta Basin

The methane and CO_2 fluxes measured in this study were used to estimate the emissions from leaking wellheads. Emissions were estimated based on well status. The Uinta Basin included wells in Uintah and Duchesne counties. The estimated emissions from producing and shut-in natural gas wells from all the measurements in this study and applied to the number of natural gas wells with producing and shut-in status in the Uinta Basin. Producing gas wells consisted of 23% of all the wells in the Uinta Basin. Shut-in

gas wells consisted of 2% of the wells. Gas storage wells are not present in the Uinta Basin; and are not included in estimated emissions. The average methane flux of shut-in gas wells was higher than producing gas wells, but because producing gas wells are more abundant, they are estimated to emit more methane from well pad soils than shut-in gas wells (Table 5). Producing and shut-in natural gas wells were estimated to emit 16.1 and 8.6 t $y^{-1}$of methane in the Uinta Basin, respectively. In 2014, the emissions from natural gas facilities in the Uinta Basin were measured by the EPA's flight tool (http://ghgdata.epa.gov/ghgp). The sum of these emissions, including the estimated emissions in the study were calculated to determine the rate and percent of emissions from producing and shut-in gas wells. The emissions were relatively small, <0.1% of natural gas emissions are sourced from producing and shut-in gas wells. Previous studies have suggested that large well leaks come from a small number of "super-emitters" (Brandt, 2014). Superemitters could increase the estimated emissions for the Uinta Basin. Sampling only 27 wells, assumptions for super-emitters were not included to estimate methane emissions.

Table 5. Estimated yearly methane and CO_2 fluxes in the Uinta Basin of producing and shut-in gas wells.

Well Status	Methane	CO_2
Producing	16.1 ± 4.3 t y^{-1}	371.0 ± 25.8 t y^{-1}
Shut-in	8.7 ± 3.2 t y^{-1}	88.0 ± 6.8 t y^{-1}

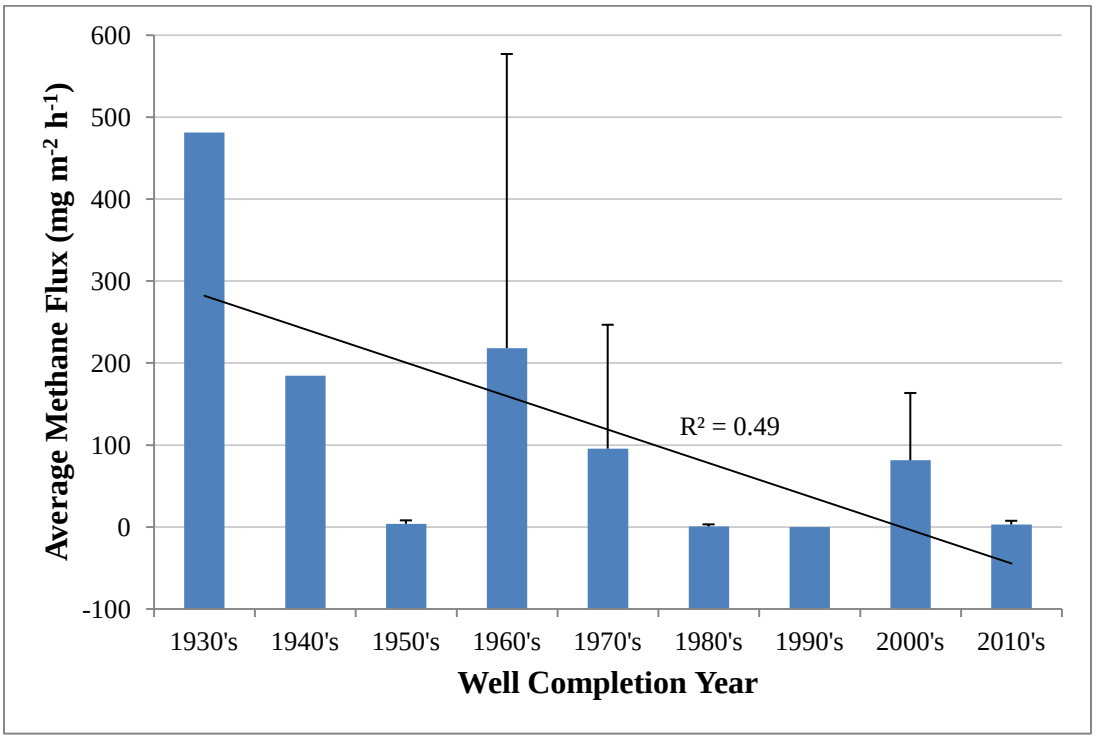

Figure 18. Average methane fluxes and well completion year by decade. Whiskers represent 90% confidence interval.

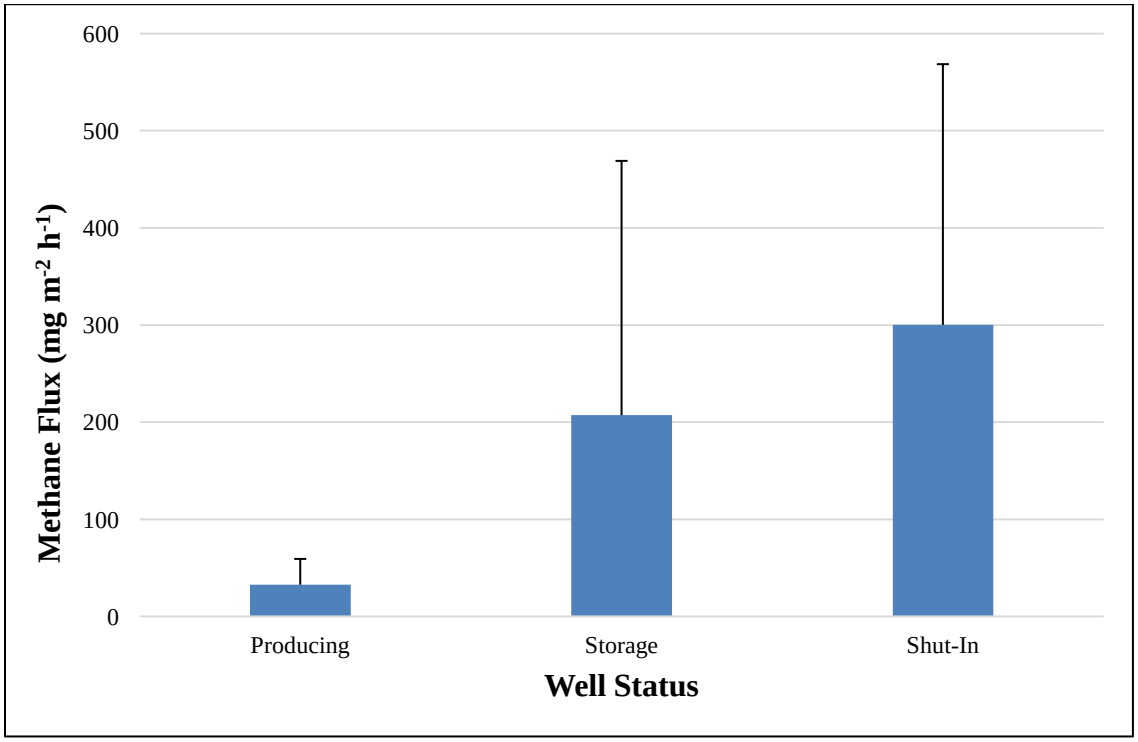

Figure 19. The average methane flux of producing, storage, and shut-in gas wells. Whiskers represent 90% confidence interval.

CHAPTER 5

SUMMARY

Hydrocarbon and CO_2 emissions from production and shut-in gas wells were estimated to contribute <0.1% of natural gas-related emissions, and therefore are not a significant source of pollution. Emissions from well pad soils do not have a major impact on air quality in the Uinta Basin. Although the emissions from well pad soils are not a significant source of pollution, measurements of these emissions were used to identify the source of emissions. More quantified measurements of hydrocarbons and CO_2 at well sites would allow better estimates of gas-related emissions. Hydrocarbon and CO_2 emissions sources were from well leaks, liquid hydrocarbon spills, and bacterial production. The majority of the emissions from wells was due to subsurface leaks of raw natural gas and was determined by the following criteria.

- Methane fluxes >10 mg m^{-2} h^{-1} were a strong indicator that a raw gas leak was present. Raw gas leaks were also identified when methane flux exceeded the NMHC flux. Among the NMHC, propane and ethane fluxes were correlated with methane fluxes. Leaks were dependent on distance and direction from the wellhead. Higher emissions were significantly correlated with distances from the wellhead. On average, the closer the measurements were to the wellhead, the higher the methane flux. Local directional subsurface leaks from the wellhead were identified with high-density DFC measurements.
- Emissions were also influenced by liquid hydrocarbon spills that contaminated the soil. Liquid hydrocarbon spills were identified when NMHC flux exceeded methane flux. Spills were also identified by heavier hydrocarbons that dominated emissions.

- A combination of raw natural gas leaking from the well and bacterial production of CO_2 from methane was measured at well sites. CO_2 fluxes were higher than methane fluxes 92% of the time.
- TOC and pH are soil properties that appear to affect methane emissions. Increased TOC and decreased pH resulted in increased methane fluxes.
- Shut-in wells are under increased pressure and were more likely to leak. Shut-in wells measured higher emissions than gas storage and producing wells.

REFERENCES

Allen, D.T., Torres, V.M., Thomas, J., Sullivan, D.W., Harrison, M., Hendler, A., Herndon, S.C., Kolb, C.E., Fraser, M.P., Hill, A.D., Lamb, B.K., Miskimins, J., Sawyer, R.F., and Seinfeld, J.H., 2013, Measurements of methane emissions at natural gas production sites in the United States: Proceedings of the National Academy of Sciences, p. 17768–17773.

Anders, D.E., Palacas, J.G., Johnson, R.C., 1992, Thermal maturity of rocks and hydrocarbon deposits, Uinta Basin, Utah, *in* Fouch, T.D, Nuccio, V.F., Chidsey, T.C.Jr., eds., 1992 Hydrocarbon and Mineral Resources of the Uinta Basin, Utah and Colorado: Salt Lake City, Utah, Utah Geological Association Guidebook 20, p. 53-76.

Baars, D. L., 2000, Geology of Canyonlands National Park: In Geology of Utah's Parks and Monuments, Sprinkel, D.A., Chidsey, T. C., and Anderson, P. B., editors, Utah Geological Association Publication 28., p. 61-83. <http://3dparks.wr.usgs.gov/coloradoplateau/canyonlands_strat.htm>.

Barbeau, D.L., 2003, A flexural model for the Paradox Basin: implications for the tectonics of the Ancestral Rocky Mountains: Basin Research, v. 15, p. 97–115.

Birdwell, J.E., Mercier, T.J., Johnson, R.C., and Brownfield, M.E., 2015, In-place oil shale resources of the Mahogany zone, Green River Formation, sorted by grade, overburden thickness, and stripping ratio, Piceance Basin, Colorado, and Uinta Basin, Utah: U.S. Geological Survey Fact Sheet 2015–3005, 6 p., <http://dx.doi.org/10.3133/fs20153005>.

Brandt, A.R., Heath, G.A., Kort, E.A., O'sullivan, F., Pétron, G., Jordaan, S.M., Tans, P., Wilcox, J., Gopstein, A.M., Arent, D. and Wofsy, S., 2014, Methane leaks from North American natural gas systems, Science, 343(6172), pp. 733-735.

Brownstein, M., 2013, A new study measures methane leaks in the natural gas industry: Environmental Defense Fund, <https://www.edf.org/blog/2013/11/14/new-study-measures-methane-leaks-natural-gas-industry>.

Chalmers, G.R. and Bustin, R.M., 2008, Lower Cretaceous gas shales in northeastern British Columbia, Part I: geological controls on methane sorption capacity, Bulletin of Canadian petroleum geology, 56(1), pp. 1-21.

Chapman, D.S., Keho, T.H., Bauer, M.S., and Picard, M.D., 1984, Heat flow in the Uinta Basin determined from bottom hole temperature (BHT) data: Geophysics, 49, p. 453–466.

Chapman, S.J. and Thurlow, M., 1996, The influence of climate on CO2 and CH4 emissions from organic soils, Agricultural and Forest Meteorology, 79(4), pp. 205-217.

Chen, T.-M., Gokhale, J., Shofer, S., and Kuschner, W.G., 2007, Outdoor Air Pollutant--Ozone Health Effects: The American Journal of the Medical Sciences, 333(4), p. 244–248, doi: 10.1097/MAJ.0b013e31803b8e8c.

Condon, S.M. and Huffman, A.C., 1997, Geology of the Pennsylvanian and Permian cutler group and Permian Kaibab limestone in the Paradox Basin, southeastern Utah and southwestern Colorado: U.S. Geological Survey Bulletin (No.2000-P).

Conley, S., Franco, G., Faloona, I., Blake, D.R., Peischl, J., and Ryerson, T.B., 2016, Methane emissions from the 2015 Aliso Canyon blowout in Los Angeles, CA, Science, 351(6279), pp. 1317-1320.

Day, S., Dell'Amico, M., Fry, R., Tousi, H.J., 2014, Field measurements of fugitive emissions from equipment and well casings in Australian coal seam gas production facilities: report to the Department of Environment, CSIRO, Australia, pp. 1–37.

Davies, R.J., Almond, S., Ward, R.S., Jackson, R.B., Adams, C., Worrall, F., Herringshaw, L.G., Gluyas, J.G. and Whitehead, M.A., 2014, Oil and gas wells and their integrity: Implications for shale and unconventional resource exploitation, Marine and Petroleum Geology, 56, pp. 239-254.

Downey, M., 2009, Oil 101: New York, NY, Wooden Table Press.

DEEDI, 2010, Leakage testing of coal seam gas wells in the Tara 'rural residential estates' vicinity, Department of Employment, Economic Development and Innovation, Brisbane, <http://www.dnrm.qld.gov.au/__data/assets/pdf_file/0011/119675/tara-leakage-csg-wells.pdf>.

Dubiel, R.F., Kirschbaum, M.A., Roberts, L.N., Mercier, T.J., and Heinrich, A., 2000, Geology and coal resources of the Blackhawk Formation in the southern Wasatch Plateau, central Utah, Geologic Assessment of Coal in the Colorado Plateau: Arizona, Colorado, New Mexico, and Utah: US Geological Survey, Professional Paper, 1625.

Duguid, A., Butsch, R.J., Loizzo, M., and Stamp, V., 2011, Collection of baseline wellbore cement data in multiple wells in the same field, Energy Procedia, 4, pp. 5130-5137.

Edwards, P.M., Young, C.J., Aiken, K., deGouw, J., Dube, W.P., Geiger, F., Gilman, J., Helmig, D., Holloway, J.S., Kercher, J., Lerner, B., Martin, R., McLaren, R., Parrish, D.D., Peischl, J., Roberts, J.M., Ryerson, T.B., Thornton, J., Warneke, C., Williams, E.J., and Brown, S.S., 2013, Ozone photochemistry in an oil and natural gas extraction region during winter--simulations of a snow-free season in the Uintah Basin, Utah: Atmospheric Chemistry and Physics, 13.17, p. 8955-8971.

Eklund, B., 1992, Practical guidance for flux chamber measurements of fugitive volatile organic emission rates, Journal of the Air & Waste Management Association, 42(12), pp. 1583-1591.

Etiope, G. and Klusman, R.W., 2002, Geologic emissions of methane to the atmosphere, Chemosphere, 49(8), pp. 777-789.

E.P.A., 2016, Oil and Natural Gas Air Pollution Standards: Implementation, <https://www3.epa.gov/airquality/oilandgas/implement.html>.

Fouch, T.D., 1975, Lithofacies and related hydrocarbon accumulations in Tertiary strata of the western and central Uinta Basin, Utah, *in*Bolyard, D.W., ed., Symposium on deep drilling frontiers in the central Rocky Mountains: Rocky Mountain Association of Geologists, p. 163-173.

Government Accountability Office (GAO), 2010, Federal oil and gas leases--opportunities exist to capture vented and flared natural gas, which would increase

royalty payments and reduce greenhouse gases, GAO-11-34 U.S. General Accountability Office Washington DC, <http://www.gao.gov/new.items/d1134.pdf.>

Hansen, W.R., 2005, The geologic story of the Uinta Mountains. Falcon Guide Helena, Montana, p. 142.

Hanshaw, B.B., and Hill, G.A., 1969, Geochemistry and hydrodynamics of the Paradox Basin region, Utah, Colorado and New Mexico: Chemical Geology, v. 4, p. 263–294.

Harder, A., 2015, EPA sets stricter standard for ozone; new limit on pollutant linked to smog draws criticism from industry groups, environmentalists: Wall Street Journal (Online) Retrieved from <http://search.proquest.com/docview/1718119710?accountid=1476>.

Helmig, D., Thompson, C.R., Evans, J., Boylan, P., Hueber, J., and Park, J.-H., 2014, Highly Elevated Atmospheric Levels of Volatile Organic Compounds in the Uintah Basin, Utah: Environmental Science & Technology Environ. Sci. Technol., 48.9, p. 4707–4715.

Hettinger, R. D., and Kirschbaum, M. A., 2002, Stratigraphy of the Upper Cretaceous Mancos Shale (upper part) and Mesaverde Group in the southern part of the Uinta and Piceance basins, Utah and Colorado: U.S. Geological Survey (No.2764).

Horvitz, L., 1985, Geochemical Exploration for Petroleum: Science, 229, p. 821–827.

Hot-head, 2009, Wellhead Testing - Xmas Tree Cavity Testing - Test HPHT Wells: Wellhead Testing, <http://hot-hed.com/services/presstest.html>.

Howarth, R.W., Santoro, R., and Ingraffea, A., 2011, Methane and the greenhouse-gas footprint of natural gas from shale formations: Climatic Change, 106.4, p. 679–690.

Jackson, R.E. and Dusseault, M.B., 2014, Gas release mechanisms from energy wellbores, In 48th US Rock Mechanics/Geomechanics Symposium, American Rock Mechanics Association.

Johnson, R. C., and Roberts, S.B., 2003, The Mesaverde total petroleum system, Uinta-Piceance Province, Utah and Colorado. Petroleum systems and geologic assessment of oil and gas in the Uinta-Piceance province, Utah and Colorado: US Geological Survey Digital Data Series DDS-69-B p. 63.

Jones, V.T., and Drozd, R.J., 1983, Predictions of oil or gas potential by near-surface geochemistry, AAPG Bulletin, 67(6), pp. 932-952.

Kang, M., Kanno, C. M., Reid, M. C., Zhang, X., Mauzerall, D. L., Celia, M. A., Chen, Y., Onstott, T. C., 2014, Direct measurements of methane emissions from abandoned oil and gas wells in Pennsylvania, Proceedings of the National Academy of Sciences of the United States of America, 111(51), 18173–18177, <http://doi.org/10.1073/pnas.1408315111>.

Karion, A., Sweeney, C., Petron, G., Frost, G., Hardesty, R.M., Kofler, J., Miller, B.R., Newberger, T., Wolter, S., Banta, R., Brewer, A., Dlugokencky, E., Lang, P., Montzka, S.A., Schnell, R., Tans, P., Trainer, M., Zamora, R., and Conley, S., 2013, Methane emissions estimate from airborne measurements over a western United States natural gas field: Geophysical Research Letters, 40.16, p. 4393-4397.

King, G.E. and King, D.E., 2013, Environmental Risk Arising From Well-Construction Failure--Differences Between Barrier and Well Failure, and Estimates of Failure Frequency Across Common Well Types, Locations, and Well Age, SPE Production & Operations, 28(04), pp. 323-344.

Kirchgessner, D. A., Piccot, D.A., and Sushma S. M., 2000, An improved inventory of methane emissions from coal mining in the United States: Journal of the Air & Waste Management Association, 50.11, p. 1904-1919.

Klusman, R.W. andJakel, M.E., 1998, Natural microseepage of methane to the atmosphere from the Denver-Julesburg basin, Colorado, Journal of Geophysical Research: Atmospheres, 103(D21), pp. 28041-28045.

Klusman, R.W., Leopold, M.E. and LeRoy, M.P., 2000, Seasonal variation in methane fluxes from sedimentary basins to the atmosphere: Results from chamber measurements and modeling of transport from deep sources, Journal of Geophysical Research, 105(D20), pp. 24-661.

Leach, M.R., 2016, Redox Chemistry: Home Page, http://www.meta-synthesis.com/webbook/15_redox/redox.php (accessed October 2016).

Leson, G., and Winer, A.M., 1991, Biofiltration: An Innovative Air Pollution Control Technology For VOC Emissions: Journal of the Air & Waste Management Association, 41.8, p. 1045–1054.

Lillis, P.G., Warden, A. and King, J.D., 2003, Petroleum systems of the Uinta and Piceance Basins–geochemical characteristics of oil types, Petroleum systems and geologic assessment of oil and gas in the Uinta-Piceance province, Utah and Colorado: US Geological Survey Digital Data Series DDS-69-B, p. 25.

Mansfield, M.L., 2014, Kerogen maturation data in the Uinta Basin, Utah, USA, constrain predictions of natural hydrocarbon seepage into the atmosphere: Journal of Geophysical Research: Atmospheres J. Geophys. Res. Atmos., 119, p. 3460–3475, doi: 10.1002/2013JD020148.

Monson, B., and Parnell, J., 1992, The origin of gilsonite vein deposits in the Uinta Basin, Utah, *in* Fouch, T.D, Nuccio, V.F., Chidsey, T.C.Jr., eds., 1992 Hydrocarbon and Mineral Resources of the Uinta Basin, Utah and Colorado: Salt Lake City, Utah, Utah Geological Association Guidebook 20, p. 257-270.

Morgan, C.D., 1999, Reservoir Characterization of the Lower Green River Formation, Southwest Uinta Basin, Utah: Utah Geological Survey (US).

Nuccio, V.F. and Condon, S.M., 1996. Burial and Thermal History of the Paradox Basin, Utah and Colorado, and Petroleum Potential of the Middle Pennsylvanian Paradox Formation: U.S. Geological Survey Bulletin (No. 2000-O).

Rice, D. D., Fouch, T.D., and Johnson, R.C., 1992, Influence of source rock type, thermal maturity, and migration on composition and distribution of natural gases, Uinta Basin, Utah, *in* Fouch, T.D, Nuccio, V.F., Chidsey, T.C.Jr., eds., 1992 Hydrocarbon and Mineral Resources of the Uinta Basin, Utah and Colorado: Salt Lake City, Utah, Utah Geological Association Guidebook 20, p. 95-110.

Picard, D., 2001, Fugitive emissions from oil and natural gas activities, Good practice guidance and uncertainty management in national greenhouse gas inventories, Intergovernmental Panel on Climate Change.

Pitman, J. K., Franczyk, K.J., and Anders, D.E., 1987, Marine and nonmarine gas-bearing rocks in Upper Cretaceous Blackhawk and Neslen Formations, eastern Uinta

Basin, Utah-- sedimentology, diagenesis, and source rock potential: American Association of Petroleum Geologist Bulletin, 71.1, p. 76-94.

Ritter, S.M., Barrick, J.E., and Skinner, M.R., 2002, Conodont Sequence Biostratigraphy of the Hermosa Group (Pennsylvanian) At Honaker Trail, Paradox Basin, Utah: Journal of Paleontology, v. 76, p. 495–517.

Panikov, N.S. and Dedysh, S.N., 2000, Cold season CH4 and CO2 emission from boreal peat bogs (West Siberia): Winter fluxes and thaw activation dynamics, Global Biogeochemical Cycles, 14(4), pp.1071-1080.

Praagman, F., Rambags, F., 2008, Migrations of natural gas through the shallow subsurface: Implications on the surveillance of low pressure pipelines, University of Utrecht.

Purdue, L.J., Dayton, D.P., Rice, J. and Bursey, J., 1991, Technical assistance document for sampling and analysis of ozone precursors, US Environmental Protection Agency and Radian Corporation (EPA-600/8-91/215).

Q.P.C., Clay Basin Cross Section Map: Questar Pipeline Company (QPC): Clay Basin Cross Section Map, (Online) Retrieved from <http://www.questarpipeline.com/html/2FrameCrossSectMaps.html>.

Q.P.C., Clay Basin Presentation: Questar Pipeline Company (QPC): Clay Basin Presentation, (Online) Retrieved from <http://www.questarpipeline.com/PPT_ClayBasin/2FrameClayBasinPresentation.html>.

Ririe, G.T. and Sweeney, R.E., 1993, Comparison of hydrocarbon gases in soils from natural seeps and anthropogenic sources, In Proceedings of the 1993 Petroleum

Hydrocarbons and Organic Chemicals in Ground Water: Prevention, Detection, and Restoration.

Sandberg, C., Holmes, J., McCoy, K. and Koppitsch, H.E.I.N.R.I.C.H., 1989. The application of a continuous leak detection system to pipelines and associated equipment, IEEE Transactions on Industry applications, 25(5), pp. 906-909.

Schnell, R. C., Oltmans, S. J., Neely, R. R., Endres, M.S., Molenar, J. V., and White, A. B., 2009, Rapid photochemical production of ozone at high concentrations in a rural site during winter: Nature Geoscience, 2.2, p. 120-122.

Selley, R.C., 1985, Elements of Petroleum Geology: New York, NY, W.H. Freeman and Company, 470 p.

Soil Survey Staff, 2009, Soil Survey Field and Laboratory Manual, USDA- Natural Resources Conservation Service.

Swanson, A.L., 2005, Trace gas emissions through a winter snowpack in the subalpine ecosystem at Niwot Ridge, Colorado: Geophys. Res. Lett. Geophysical Research Letters, v. 32.

Sweeney, J. J., Burnham, A.K., and Braun, R.L., 1983, A model of hydrocarbon generation from type I kerogen--application to Uinta Basin, Utah: American Association of Petroleum Geologist Bulletin, 71.8, p. 967-985.

Thielemann, T., Lücke, A., Schleser, G.H. and Littke, R., 2000, Methane exchange between coal-bearing basins and the atmosphere: the Ruhr Basin and the Lower Rhine Embayment, Germany. Organic Geochemistry, 31(12), pp. 1387-1408.

Tissot, B., Deroo, G., and Hood, A., 1978, Geochemical study of the Uinta Basin: formation of petroleum from the Green River formation: Geochimica et CosmochimicaActa, v. 42, p. 1469–1485.

Topp, E. and Pattey, E., 1997, Soils as sources and sinks for atmospheric methane, Canadian Journal of Soil Science, 77(2), pp. 167-177.

Utah Dept. of Administrative Services: Office of Administrative Rules, 2016, Utah Department of Administrative Services Office of Administrative Rules: UT Admin Code R649-2. General Rules. October 1, 2016, <http://www.rules.utah.gov/publicat/code/r649/r649-002.htm> (accessed October 2016).

Walton, P.T., 1944, Geology of the Cretaceous of the Uinta Basin, Utah: Geological Society of America Bulletin, v. 55, p. 91–130.

Wang, D.K.W. and Austin, C.C., 2006, Determination of complex mixtures of volatile organic compounds in ambient air: canister methodology, Analytical and bioanalytical chemistry, 386(4), pp. 1099-1120.

Warmuzinski, K., 2008, Harnessing methane emissions from coal mining, Process Safety and Environmental Protection, 86(5), pp. 315-320.

Xu, L., Lin, X., Amen, J., Welding, K. and McDermitt, D., 2014, Impact of changes in barometric pressure on landfill methane emission, Global Biogeochemical Cycles, 28(7), pp. 679-695.

APPENDICES

Appendix A: 56 NMHC

Table A1. List of the 56 non-methane hydrocarbons analyzed.

Chemical Compound	Formula
Ethane	C_2H_4
Ethylene	C_2H_2
Propane	C_2H_6
Propylene	C_3H_6
Iso-butane	C_3H_8
N-butane	C_4H_{10}
Acetylene	C_4H_8
Trans-2-Butene	C_4H_{10}
1-Butene	C_4H_8
Cis-2-butene	C_4H_8
isopentane	C_5H_{10}
n-pentane	C_5H_{12}
trans-2-pentene	C_5H_8
1-pentene	C_5H_{10}
cis-2-pentene	C_5H_{10}
2,2-dimethylbutane	C_6H_{14}
cyclopentane	C_5H_{10}
2,3-dimethylbutane	C_6H_{14}
2-methylpentane	C_6H_{14}
3-methylpentane	C_6H_{14}
Isoprene	C_6H_{14}
1-Hexene	C_6H_{12}
n-Hexane	C_6H_{14}
Methylcyclopentane	C_6H_{12}
2,4-Dimethylpentane	C_7H_{16}
Benzene	C_6H_6
Cyclohexane	C_6H_{12}
2-Methylhexane	C_7H_{16}
2,3-Dimethylpentane	C_7H_{16}
3-Methylhexane	C_7H_{16}
2,2,4-Trimethylpentane	C_8H_{18}
n-Heptane	C_7H_{16}
Methylcyclohexane	C_7H_{14}
2,3,4-Trimethylpentane	C_8H_{18}
Toluene	C_7H_8
2-Methylheptane	C_8H_{18}
3-Methylheptane	C_8H_{18}

n-Octane	C_8H_{18}
Ethylbenzene	C_8H_{10}
m-Xylene	C_8H_{10}
p-Xylene	C_8H_{10}
Styrene	C_8H_8
o-Xylene	C_8H_{10}
n-Nonane	C_9H_{20}
Isopropylbenzene	C_9H_{12}
n-Propbylbenzene	C_9H_{12}
m-Ethyltoluene	C_9H_{12}
p-Ethyltoluene	C_8H_{12}
1,3,5-Trimethylbenzene	C_9H_{12}
o-Ethyltoluene	C_9H_{12}
1,2,4-Trimethylbenzene	C_9H_{12}
n-Decane	$C_{10}H_{22}$
1,2,3-Trimethylbenzene	C_9H_{12}
m-Diethylbenzene	$C_{10}H_{14}$
p-Diethylbenzene	$C_{10}H_{14}$
n-Undecane	$C_{11}H_{24}$

Appendix B. Tables

Appendix B1. Annual and total combustible soil gas (ppm) of each well with measurements taken ≤1.5 meters (5 ft) from the wellhead. Whiskers represent a 90% confidence interval.

Well Name	Summer 2013 Average Soil Gas	Summer 2014 Average Soil Gas	Summer 2015 Average Soil Gas	Summer 2016 Average Soil Gas	Total Average Soil Gas
MIDDLE MESA FED 25-41-29-24			85,994 ± 104,676		85,994 ± 104,676
BULL HORN FED 15-14-30-25		520,000	280 ± 238		208,168 ± 271,395
BULL HORN FED 9-14-30-25		2,540 ± 8,082			2,540 ± 8,082
RW 34-22C	6,590 ± 40,471		203,500 ± 245,618	620,000 ± 307,640	281,289 ± 176,556
RW 32-22B	5,330 ± 15,595	9,240	5,180 ± 7,447	565	5,137 ± 2,673
RW 21-22B	9,100	2,980 ± 12,753	16,287 ± 12,372	2,301 ± 2,562	8,308 ± 5,079
RW 5C1-23B		70 ± 63	169 ± 89		129 ± 63
RW 12B1-23B		20 ± 126	172 ± 86		111 ± 88
CWU 1362-25			26,129 ± 43,510		26,129 ± 43,510
OU GB 3W-20-8-22			61,865 ± 64,710	96,677 ± 213,447	73,469 ± 56,054
CLAY BASIN UNIT 12	128,000 ± 707,140	605,000 ± 852,356	165,000 ± 726,081	76,000 ± 176,428	243,500 ± 170,854
CLAY BASIN UNIT 7			837,500 ± 101,393	366,667 ± 145,349	635,714 ± 193,663
CLAY BASIN UNIT 54-S		170,000	225,186 ± 529,361	243 ± 413	133,934 ± 211,122
CLAY BASIN UNIT 2		32,000 ± 40,958			32,000 ± 40,958
CLAY BASIN UNIT 19	115,000 ± 726,081				115,000 ± 726,081
CLAY BASIN UNIT 23	2,600 ± 16,416				2,600 ± 16,416

Appendix B2. Coordinates and the number of DFC locations of each hydrocarbon-bearing outcrop.

Hydrocarbon-bearing Outcrop	# of Measurements	Average Methane Flux	Latitude	Longitude
Coal	2	0.01 ± 0.05	40.27969	-109.06600
Coal	2		40.28616	-109.13000
Gilsonite	4	-0.07 ± 0.02	39.84592	-109.19003
Oil Shale	2	0.02 ± 0.02	39.87516	-109.15513
Oil Shale	2		39.88235	-109.15872
Fault Zone	2	0.07 ± 0.16	40.34423	-109.31073

Appendix C. Figures

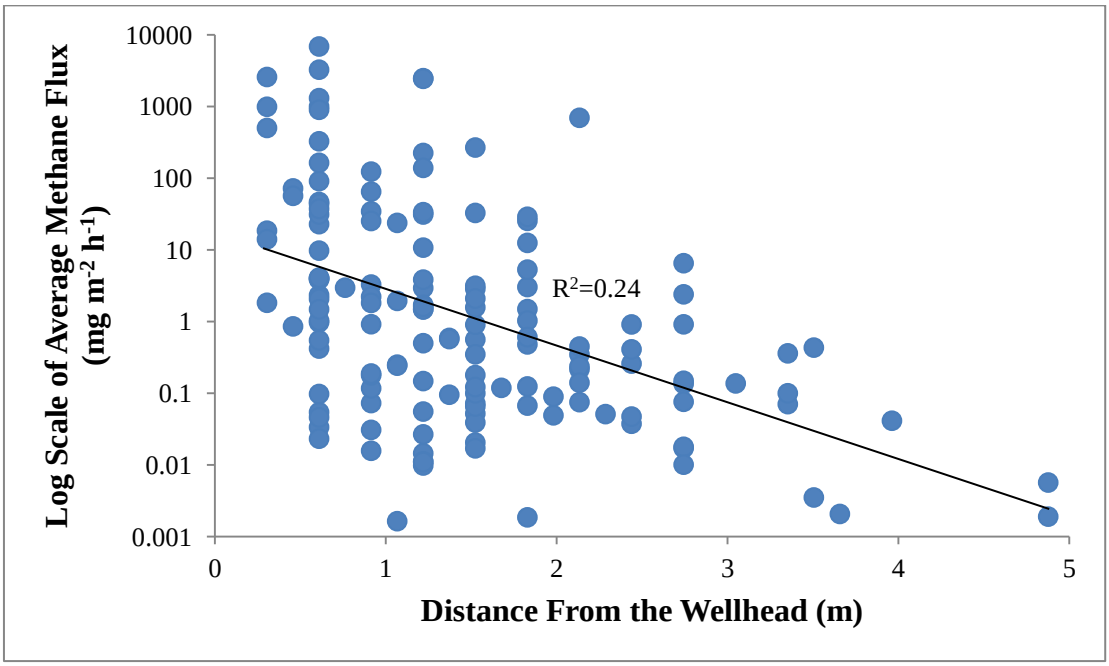

Appendix C1. Methane flux and distance from the wellhead with logarithmictrend correlation.

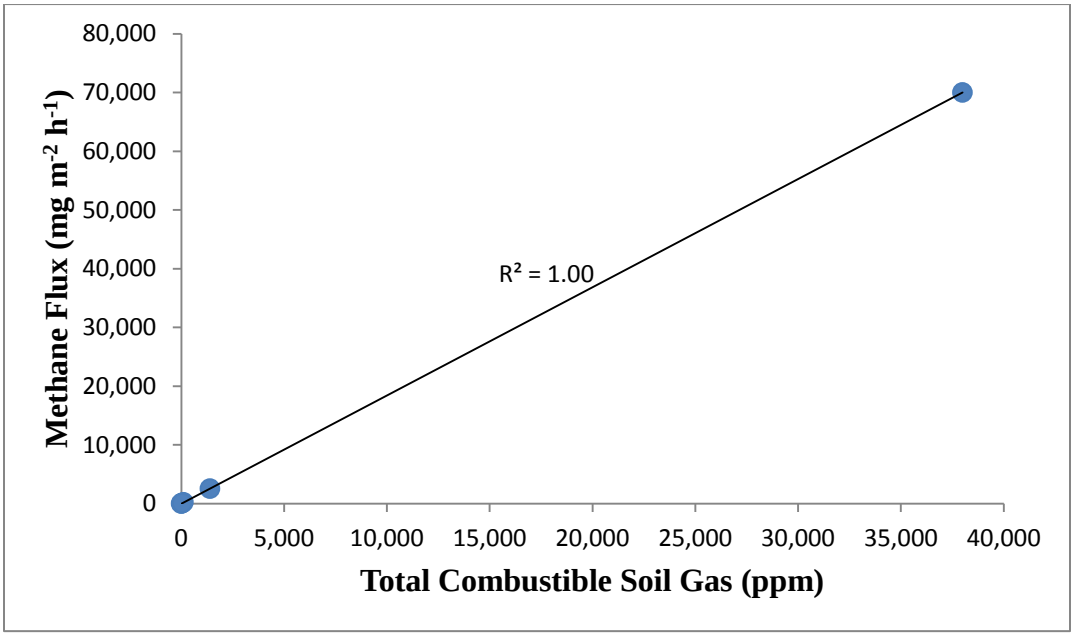

Appendix C2. Total combustible gas and methane flux correlation. Total combustible soil gas was projected to estimate a methane flux of 70,000 ppm.